Journal of Structural Geology 139 (2020) 104129

Contents lists available at ScienceDirect

Journal of Structural Geology

journal homepage: http://www.elsevier.com/locate/jsg

Transformation weakening: Diffusion creep in eclogites as a result of interaction of mineral reactions and deformation

H. Stünitz [a,b,*], K. Neufeld [a], R. Heilbronner [a,c], A.K. Finstad [a], J. Konopásek [a,d], J.R. Mackenzie [c,1]

[a] Dept. of Geosciences, University of Tromsø, Dramsveien 201, 9037, Tromsø, Norway
[b] Institut des Sciences de la Terre (ISTO), Université d'Orléans, 1a Rue De La Férollerie, 45071, Orléans, Cedex 2, France
[c] Geological Institute, Bernoullistr. 32, CH-4056, Basel, Switzerland
[d] Czech Geological Survey, Klárov 3, 118 21, Prague, 1, Czech Republic

A B S T R A C T

The deformation of eclogites and the driving forces for their fabric development are an important topic, potentially allowing to determine deformation rates and stresses in subduction zones, where the greatest number of large earthquakes occurs. Here, fabric studies of grain size and shape, texture, and chemical composition from two locations of Variscan and Alpine eclogites are presented. All samples show a well-developed crystallographic preferred orientation (CPO) of omphacite with a strong maximum of [001] in the lineation direction and a weaker maximum of poles to (010) normal to foliation. Garnet shows no systematic CPO. Anisotropic chemical zoning developed in omphacite and garnet during growth together with elongated grain shapes and can be related to a prograde (in terms of pressure change) P,T-path. The individual chemically zoned and elongated grains orientated in the stretching direction are single crystals without major internal misorientations. Chemical, microstructural, and CPO data indicate that the deformation microstructure and texture were produced by preferential crystal growth of garnet and omphacite grains in the extension direction. Dislocation creep can be excluded as a possible fabric formation process by the systematic and oriented chemical zonation of single crystals and absence of dynamic recrystallization microstructures. The dominant deformation is inferred to be diffusion creep, where dissolution of material took place in reacting mafic phases (plagioclase, pyroxene) and precipitation took place in the form of new eclogite facies minerals (omphacite, garnet, zoisite). This type of diffusion creep deformation represents a transformation process involving both, deformation and metamorphic reactions. It is emphasized that the weakening is directly connected to the transformation and therefore transient. The weakening facilitates diffusion creep deformation of otherwise strong minerals (pyroxene, garnet, zoisite) at far lower stresses than dislocation creep. The results imply low stresses during the deformation of eclogite blocks in subduction zones. These results can be applied to other rock types, too.

1. Introduction

Subduction zones are very large thrust faults, in which seismogenic and aseismic sections can be distinguished (including slow slip phenomena; Gomberg et al., 2007), usually based on the degree of coupling along the plate interface (e.g., Pacheco et al., 1993; Hyndman et al., 1997; Agard et al., 2018). The parameters defining the degree or extent of coupling may include temperature, rock composition, fluid pressure, etc. (Agard et al., 2016). The most critical parameter is the rheology of the deforming material at the plate interface (e.g. Stöckhert and Renner, 1998; Agard et al., 2018, and references therein). The rheology will depend primarily on the lithology and temperature of the deforming volume of the rock, the displacement rates being similar (one to several cm/a) in most subduction zones. One type of rock involved in many subduction zones is the mafic oceanic crust, which undergoes mineral reactions to form eclogites.

The formation and development of mineral fabrics in eclogites is an important problem in tectonics, because microstructural studies are used as indicators for deformation and exhumation processes under (ultra)-high-pressure conditions (e.g. Keppler, 2018). The main mechanisms for fabric development and thus the deformation mechanisms in eclogite-facies rocks are an ongoing matter of debate and topic of numerous studies. Based on the analysis of crystallographic preferred orientation (CPO), previous studies have focused on discussions of whether dislocation creep or diffusion creep give rise to fabric formation and development. It is often assumed that only crystal plastic deformation affects and leads to the formation of a CPO, implying that dislocation creep has to be the most important fabric forming process. Regarding eclogite minerals, previous studies of fabric development focused strongly on omphacite while garnet studies are comparatively rare.

* Corresponding author. Dept. of Geosciences, University of Tromsø, Dramsveien 201, 9037, Tromsø, Norway.
E-mail address: holger.stunitz@uit.no (H. Stünitz).
[1] Deceased

https://doi.org/10.1016/j.jsg.2020.104129
Received 11 October 2019; Received in revised form 26 June 2020; Accepted 27 June 2020
Available online 9 July 2020

Helmstaedt et al. (1972) distinguished two main types of omphacite CPO in eclogites: (1) A c-axis maximum parallel to lineation and b-axis girdle in L-tectonites, and (2) A b-axis maximum and c-axis girdle in S-tectonites. The CPO is interpreted to be the result of syndeformational recrystallization in the solid state related to growth and shape preferred orientation (SPO). The different types of CPO pattern reflect deformation in the constriction or flattening strain field, an interpretation supported by Godard and van Roermund (1995) and Abalos (1997). Bascou et al. (2001, 2002) performed viscoplastic self-consistent (VPSC) modelling arguing that different deformation regimes are reflected in the observed CPO patterns consistent with the activation of observed slip systems in dislocation glide for omphacite. A different view is presented by Brenker et al. (2002), who has discussed that S- and L-type CPO fabrics might be formed depending on cation ordering of omphacite defined by its formation temperature and would therefore be independent of any deformation processes. From this very short summary it is obvious that deformation and fabric forming processes are not clear for eclogites.

Slip systems in omphacite have been determined to be [001](100), [001]{110}, ½ <110>{110}, and ½ [100](010) by van Roermund and Boland (1981), van Roermund (1983, 1984), Buatier et al. (1991), Phillipot and van Roermnund (1992), Godard and van Roermund (1995), Rehman et al. (2016). Slip systems are partly different from other clinopyroxenes, see references in Godard and van Roermund (1995).

Garnet deformation by dislocation creep was inferred by Kleinschrodt and McGrew (2000), Massey et al. (2011), and Storey and Prior (2005). Mainprice et al. (2004) discussed plastic deformation in garnets by comparing laboratory experiments with naturally deformed eclogites and suggested that garnet fabrics can be affected by plastic deformation at very high pressures and temperatures (ultrahigh-pressure conditions). Diffusion creep was inferred for the deformation of garnet by Storey and Prior (2005), Massey et al. (2011), and Smit et al. (2011).

Bons and den Brok (2000) presented a general numerical model demonstrating that, in contrast to dislocation creep in rocks, reaction-controlled dissolution-precipitation creep may form a CPO in deformed rocks. Mauler et al. (2001) argued for a process of eclogite deformation based on dissolution and anisotropic growth (pressure solution creep) with grain boundary diffusion as rate-controlling factor based on CPO studies of omphacites in eclogites from the Armorican Massif. Diffusion creep as a subordinate mechanism is discussed by Godard and van Roermund (1995). Most authors, however, favor dislocation creep to be the principal process causing the fabric development because strong CPOs have been observed in naturally deformed eclogites (Phillipot and van Roermund (1992), Godard and van Roermund (1995), Abalos (1997), Kurz et al. (1998, 2004), Abalos et al. (2003), Mainprice et al. (2004), Kurz (2005), Neufeld et al. (2008), Keppler et al. (2015, 2016), Rehman et al. (2016), and Collett et al. (2017)).

The deformation mechanisms and rheology of mafic rocks, eclogites, and their main constituents have been studied experimentally by, e.g., Dimanov and Dresen (2005), Dimanov et al. (2003, 2007), Orzol et al. (2003), Zhang et al. (2006), Moghadam et al. (2010). The general conclusions in all of these studies is that clinopyroxene is a strong mineral and deformation by dislocation creep should occur only at high differential stresses at geologically realistic temperatures of 550–750 °C, typical for high pressure rocks in subduction zones. Some of the stresses required for dislocation creep are concluded to be unrealistically high for natural conditions (Moghadam et al., 2010).

To investigate the deformation mechanisms in eclogites in more detail and to test previous models, this study analyses the relation between the development of chemical zonation, shape fabrics and CPO in garnet and omphacite in samples of mafic eclogites in order to determine the dominant processes for fabric formation in these rocks. Variscan and Alpine eclogites from two different locations were studied to analyze a range of (micro)structural settings. The main focus lies on Saxothuringian eclogites from the Variscan Bohemian Massif (Czech Republic). These show a pronounced elongated shape of both garnet and omphacite crystals and are therefore ideal for a study of the relation between grain shape, chemical and CPO development. The results are compared with a sample from the Tauern Window as it is similar in P,T conditions, though partly different in grain size and shape. The Eclogite Zone in the Tauern Window is also a key study area for a number of papers discussing eclogite fabric formation (Kurz et al., 1998, 2004; Kurz, 2005; Neufeld et al., 2008; Keppler et al., 2015, 2016). Therefore, our two sets of samples provide an opportunity to compare our results with previous models.

1.1. Geological settings

1.1.1. Bohemian Massif

The structures and metamorphism of the Bohemian Massif are the result of the closure of the Saxothuringian Ocean during Devonian subduction and subsequent early Carboniferous continent-continent collision (e.g. Matte et al., 1990; Franke, 2000; Schulmann et al., 2009). Samples for this study come from the Saxothuringian domain (Hoth et al. (1983); Kossmat, 1927; Hoth et al. (1983); Franke, 2000), which represents the lower plate of the collisional system and contains remnants of high-pressure rocks exhumed from a subduction channel (O'Brien, 2000; Masur and Aleksandrowski, 2001; Konopásek and Schulmann, 2005; Schulmann et al., 2009, 2014; Jeřábek et al., 2016). The Saxothuringian mafic eclogites are exposed in the Erzgebirge Mountains and occur in association with high-to ultra-high-pressure metasedimentary rocks (Rötzler et al., 1998; Konopásek, 1998, 2001; Nasdala and Massone, 2000) and metagranitoids (Kotková, 1993; Willner et al., 1997; Kotková et al., 2011). Different peak metamorphic conditions in individual eclogite bodies indicate that the Erzgebirge mafic eclogites were exhumed from different depths of the subduction channel (Schmädicke et al., 1995).

The subduction-related rocks show similar metamorphic- and cooling ages indicating a fast exhumation rate (Zulauf et al., 2002; Konopásek and Schulmann, 2005). The peak metamorphic conditions during the formation of the eclogite samples used in this study have been estimated to be ~600–700 °C and 2.5–2.6 GPa by Klápová et al. (1998) and Collett et al. (2017).

1.1.2. Tauern Window

The Tauern Window (Eastern Alps, Austria) exposes rocks of the European plate together with Penninic units below the Austroalpine nappes in the Eastern Alps (e.g., Schmid et al., 2013, and references therein). From top to bottom it consists of the Penninic Glockner Nappe with rocks of oceanic affinity that reached blueschist facies metamorphic conditions of ~0.8 GPa, 500 °C, the Eclogite Zone, and the Venediger Nappe, comprising gneisses and parauthochtonus metasediments with peak metamorphic conditions of ~1.1 GPa, 540 °C (e.g Selverstone, 1993; Kurz et al., 1998, 2004; Schmid et al., 2004, 2013). The Eclogite Zone (EZ) is located in the southern part of the Tauern Window, with thrust contacts to the Glockner Nappe above and Venediger Nappe below. The EZ crops out along a strike length of ~20 km in E-W direction with variation in its N-S extent between 1.5 and 3 km. The eclogite blocks occur as lenses with a size up to 1500 × 700 m and are embedded in a matrix of more deformed and mylonitic garnet mica schists, marbles and quartzites. Eclogite bodies make up ~30% of the overall Eclogite Zone (Neufeld et al., 2008). Peak metamorphic conditions have been determined as 2.5 GPa and 600° ± 30 °C (Stöckhert et al., 1997; Hoschek, 2001, 2007), i.e. similar to those of the Bohemian massif samples. A rapid exhumation rate of at least 36 mm yr^{-1} was suggested by Glodny et al. (2005).

2. Analytical methods

All samples are polished thin sections of hand specimens cut both parallel and perpendicular to the XZ plane of the fabric (sections parallel

Table 1
Sample coordinates and outcrop names for studied Bohemian Massif eclogites.

Sample	outcrop	coordinates	
M-1	Meluzína	N 50°23,434′	E 13°00,391′
M-6	Meluzína	N 50°23,392′	E 13°00,625′
M-7	Na skalách	N 50°23,112′	E 012°59,704′

and normal to lineation and normal to foliation). Chemical composition and zonation of garnet and omphacite crystals were analyzed using a Zeiss Merlin VP Compact scanning electron microscope (SEM) at the University of Tromsø, equipped with an energy dispersive x-ray spectroscopy (EDS) X-max 80 mm^2 system and a Nordlys electron backscattered diffraction (EBSD) detector, both by Oxford instruments, combined with the analytical software AZtec. EDS line scan analyses were run at 20 kV using a 60 μm aperture. Beam current was measured and analyses are quantitative. Backscatter electron images (BSE) were used to visualize the chemical zonation.

Orientation images were acquired by electron backscatterred diffraction (EBSD) at a tilt angle of 70° and an acceleration voltage of 20 kV. Using a stepsize of 7 or 8 μm, stitched large area maps (0.35–0.7 cm^2, 65–90% indexing) were prepared for bulk pole figure calculations. A stepsize of 0.2–0.8 μm was used to obtain high resolution maps (80–90% indexing) of selected garnet and omphacite grains. The MTEX toolbox (Hielscher and Schaeben, 2008) was used to calculate area weighted pole figures of garnet omphacite and hornblende for the large area maps (resolution of maps not being sufficient for grain weighted pole figures). Misorientation images (mis2mean) were calculated for the detail maps showing misorientation angles of $\ll 1°$ to demonstrate the single crystal nature of grains.

Shape fabrics were analyzed by applying the SURFOR method (Panozzo, 1984; Heilbronner and Barrett, 2014) on samples from the Meluzina eclogites. Phase maps were obtained for garnet, omphacite and quartz by thresholding and grey level slicing of BSE contrast SEM images using ImageJ. Grain maps were obtained by further manual segmentation. On x-z sections (parallel to lineation), the outlines of ~360–540 garnet and ~1700 to 2500 omphacite grains were digitized, and on y-z sections (normal to lineation), those of ~40–100 garnet and ~660 to 760 omphacite grains. Grain size distributions (diameters of area equivalent circles) of garnet and omphacite were determined using the Analyze menu of ImageJ. The stripstar program was used to convert to volume weighted distributions of 3D grain size (diameters of volume equivalent spheres).

Contact frequencies of grains were measured as line length, i.e., surface proportion of grain (A-A, B-B) and phase (A-B) boundaries where phase A and B could be garnet, omphacite or quartz, or B could be all

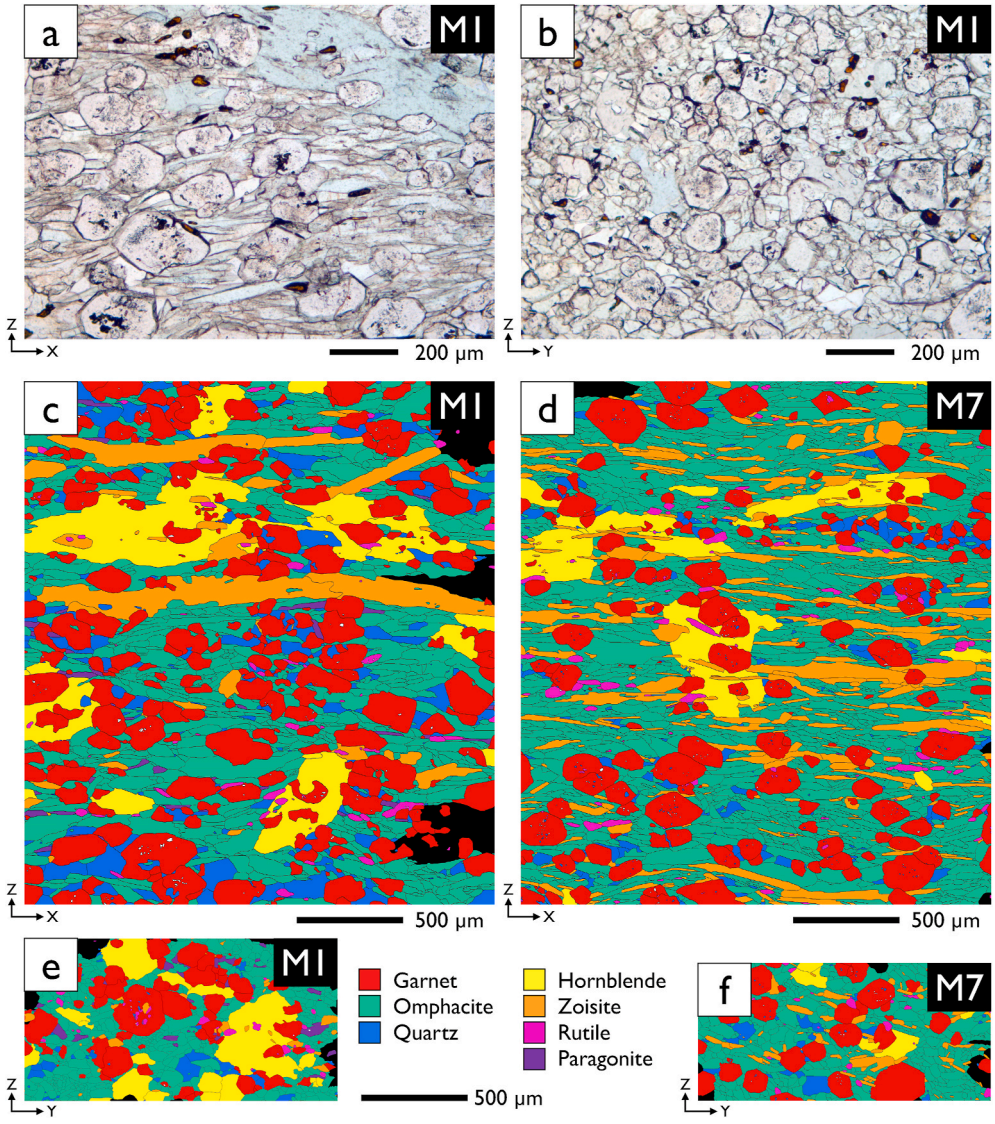

Fig. 1. Microstructures of the Bohemian massif eclogites. (a) & (b) Light micrographs of M1 parallel and normal to lineation. (c)–(f) Phase maps derived from EBSD and BSE images, parallel and normal to lineation for M1 and M7.

Table 2
Modal composition of eclogites. (in sample names: L = parallel to lineation = XZ-section, P = perpendicular to lineation = YZ-section), after Finstad (2017).

Mineral	M1-L (%)	M1-P (%)	M7-L (%)	M7-P (%)	M1 (%)	M7 (%)	EK-H
quartz	11.82	3.98	3.72	4.42	7.06	4.08	7.07
paragonite	1.32	2.90	0.02	0.00	2.01	0.00	4.06
omphacite	38.19	43.93	51.34	53.23	42.14	52.59	37.89
hornblende	9.13	19.35	6.36	3.65	13.68	4.85	6.79
zoisite	6.36	2.78	14.48	9.73	4.33	11.94	3.24
garnet	31.95	25.50	22.23	27.56	29.37	24.91	14.94
rutile	1.22	1.56	1.86	1.41	1.42	1.63	1.02
plagioclase							17.05
kyanite							7.94
TOTAL	100	100	100	100	100	100	100

phases but A (see Heilbronner & Barret, 2014; chap. 18). Frequencies are plotted versus surface fractions of phase A and B together with the binomial curve for random distributions. If the frequency of A-B boundaries lies on the curve, the spatial distribution of A and B is random, if it plots above the curve, the distribution is ordered, if it plots below the curve, the distribution is clustered. Phase content was calculated for surface proportion (corresponding to volume proportion). In addition, the individual grain maps of garnet, omphacite and quartz and the combined phase maps of garnet and quartz were subjected to an analysis by the autocorrelation function (ACF).

3. Results

3.1. Microstructures and shape fabrics

3.1.1. Eclogites from the Erzgebirge, Bohemian Massif

Several samples were taken from the Meluzína and Na skalách (Table 1) eclogite bodies of the Bohemian massif (Klápová et al., 1998), and three (M1, M6, M7) were investigated in detail. They are fine grained eclogites dominated in their modal mineral composition by garnet and omphacite (Fig. 1, Table 2). Parallel to lineation all samples show elongated grain shapes (especially omphacite, garnet, and zoisite) that constitute the lineation and general extension direction in these rocks (XZ-section; Fig. 1). Omphacite grain shapes in the XZ section have a higher aspect ratio (from SURFOR analysis) of ~2.2–2.5 than those of garnet (~1.4; Fig. 2a). The modal abundance has been determined in

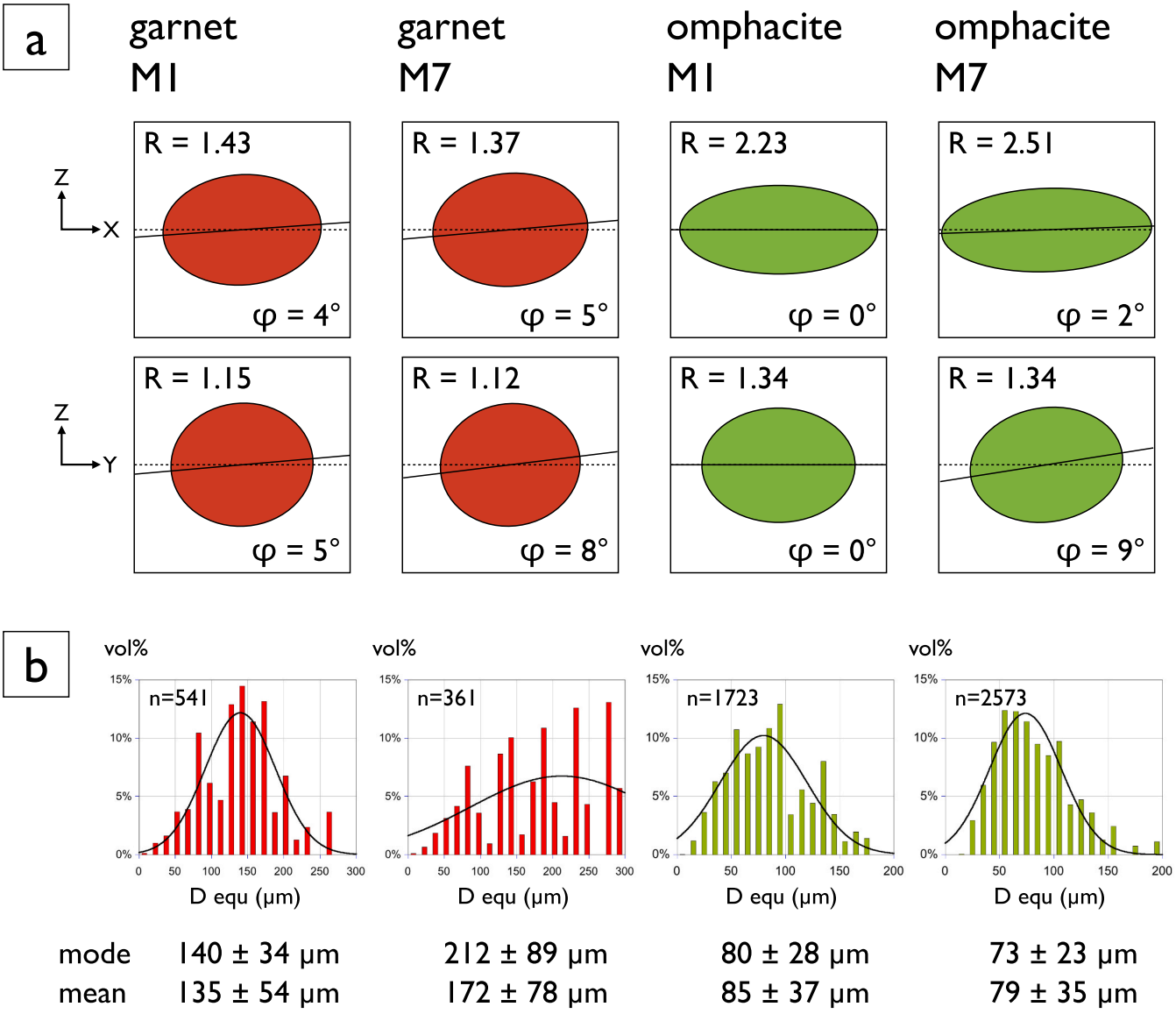

Fig. 2. Shape and grain size analysis of Bohemian massif eclogites.(a) Characteristic shapes derived from SURFOR analysis for garnet and omphacite of M1 and M7. (b) STRIPSTAR derived 3D grain size distributions of garnet and omphacite of M1 and M7: volumetric density against the equivalent diameter of the 3D grains. Mean diameters and modes of Gauss fits are indicated.

sections parallel and normal to lineation, and the different modal percentages are partially a function of mineral shapes (e.g., rod-shapes for zoisite). The average percentages are given in Table 2: In addition to garnet (~25–30%) and omphacite (~40–50%), the mineral assemblage includes quartz, zoisite, and amphibole, as well as trace amounts of rutile and paragonite.

Omphacite represents the larger part of the matrix surrounding the garnet grains. The 3D-mode of the grain sizes of the garnet is ~140–210 μm, that of omphacite between ~75 and ~80 μm (Fig. 2b). YZ-sections show more isotropic grain shapes (aspect ratios garnet ~1.1–1.15, omphacite ~1.35; Fig. 2a). The fabric anisotropy of characteristic grain shapes (from SURFOR data) plot near the k = 1 line for garnets and clearly in the uniaxial prolate fabric field for omphacite (Fig. 3).

Zoisite occurs as elongated prismatic to tabular crystals with their long axes oriented parallel to lineation and their shortest axis near normal to the foliation (Fig. 1). Rutile is randomly distributed in the samples. Amphiboles can be elongated, but their long axes have a more or less random orientation in all sections because ampiboles overgrow the rock fabric as a postkinematic mineral (Fig. 1). Diopside and plagioclase symplectites with a maximum grain size of 5 × 2 μm may occur in cracks and at grain boundaries of omphacite grains in all three samples. Their modal abundance typically is far lower than 10% and has not been considered in the modal mineral analysis.

3.1.2. Eclogite from the Tauern Window, Austrian Alps

Of the samples taken from several Tauern window locations, several were studied in detail, and for this paper, sample EK-H was selected for documentation. It represents a fine grained to mylonitic eclogite, which is typical for the Eclogite Zone (EZ). The sample is foliated and shows a well-developed stretching lineation which is parallel to the stretching lineation of the garnet mica schists that surround the eclogite lenses within the EZ. Garnets (~15% of the sample; Table 2) occur in layers within an omphacite matrix and vary in shape. Some grains are strongly elongated in the extension direction. This elongation is parallel to that of the omphacite grains. Equant shaped garnet grains are present, too. The garnet grain size varies significantly between ~100 and ~800 μm. Omphacite grains (~40%) form a well-developed lineation and show a relatively homogeneous grain size of ~400–600 x 100–200 μm. Further mineral components are quartz, glaucophane, zoisite, kyanite, phengite, rutile and paragonite as well as hornblende and plagioclase which are related to retrogression during exhumation. While glaucophane

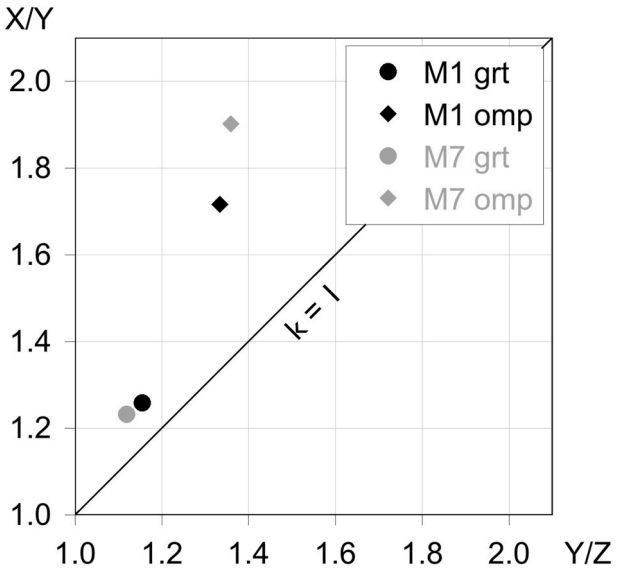

Fig. 3. Flinn diagram for Bohemian massif eclogites. Data of M1 (black) and M7 (grey) of grain shapes for garnet (circles) and omphacite (rhombs). Aspect ratios are derived from SURFOR analyses.

generally occurs as rims around the garnets, other accessory phases are distributed randomly within the sample.

3.2. Chemical composition and zonation of garnet and omphacite

The garnet and omphacite microstructures in many of the Meluzina and Tauern window samples resemble each other, and the zonation patterns are very similar in all the samples that were studied. Two of the Meluzina and one of the Tauern window samples were selected for detailed documentation here, because they are representative and show the best and most complete examples of the features of interest.

Garnets in the Bohemian Massif samples show cores with quartz inclusions. Small inner cores are generally more equant than the fully grown grains (Figs. 4 and 5). The part surrounding the cores shows a higher Mg-, lower Ca-, and decreasing Fe-content, followed by an outer rim with distinctly lower Ca- and Fe-, and increased Mg-content. Some zonation patterns have faceted shapes (Fig. 4), others are more irregular (Fig. 5). The concentric zonation pattern follows the elongated grain shape, where the final shape is more elongated than the inner parts. The grains are zoned with the compositional range stretched over a larger distance in the direction parallel to elongation than in the direction perpendicular to it, but the same zonation range is complete in all directions, i.e., the patterns usually are not truncated normal to the elongation direction - this is particularly clear in the YZ sections (Fig. 6). Most garnet grains show healed cracks expressed as narrow zonation sutures. The regions near these healed cracks in the cores show more patchy internal zonation patterns. These cracks can cut through the grains from rim to cores, so that they must have formed at the end of or after garnet growth.

Omphacite shows an even more pronounced difference in spatial distribution of chemical zonation (for long versus short axis of grains). The innermost cores invariably are Al-poor and Ca-rich (Figs. 5 and 7). In some cases the Na- and Al-contents increase from core to rim, whereas Mg and Ca-contents decrease. In other cases Ca- and Mg-contents seem to oscillate, and Na-content is slightly patchy to rather even (Fig. 7). Some cores have high aspect ratios whereas others can be more equant. This kind of garnet and omphacite zonation is typical for all samples throughout the studied sample set.

Garnet and omphacite in eclogite samples from the Tauern Window show a similar type of chemical zonation as the samples from the Bohemian Massif. Elongated garnet crystals observed in the sample EK-H also show zonation with increasing Mg-content from core to rim, coupled with decreasing Fe-content, while Ca-content decreases towards the rim (Figs. 5 and 8). The zonation patterns and outlines tend to be more faceted than the Bohemian garnets (Figs. 5, 6 and 8). There is no truncation of the patterns in the direction normal to lineation. Some omphacite crystals from the Tauern Window eclogites show the same asymmetric distribution of chemical zonation with decreasing Ca- and Mg-contents from core to rim accompanied by a slight increase in Na- and Al-contents (Fig. 5). Others show a more oscillatory zoning in Mg and Ca, but Al and Na invariably are low in the core (Fig. 9). Most Tauern omphacite cores are elongated (Figs. 5 and 9). The zonation pattern is present in all sections, with larger spacing of the compositional range of zonation parallel to the lineation and smaller spacing normal to lineation.

3.3. Crystallographic preferred orientation (CPO)

Crystallographic preferred orientations (CPO) of garnet and omphacite in all Bohemian and Tauern samples were measured in relatively large areas (0.35–0.7 cm^2, comprising up to 100′000 grains). Omphacite CPO's in eclogites from the Bohemian Massif show an orthorhombic symmetry with poles to {001} parallel to lineation. There is a very weak tendency towards a single girdle distribution of the normal to {001} in the foliation in sample M7 (Fig. 10). Poles to {010} are preferentially aligned normal to the foliation with a weak tendency

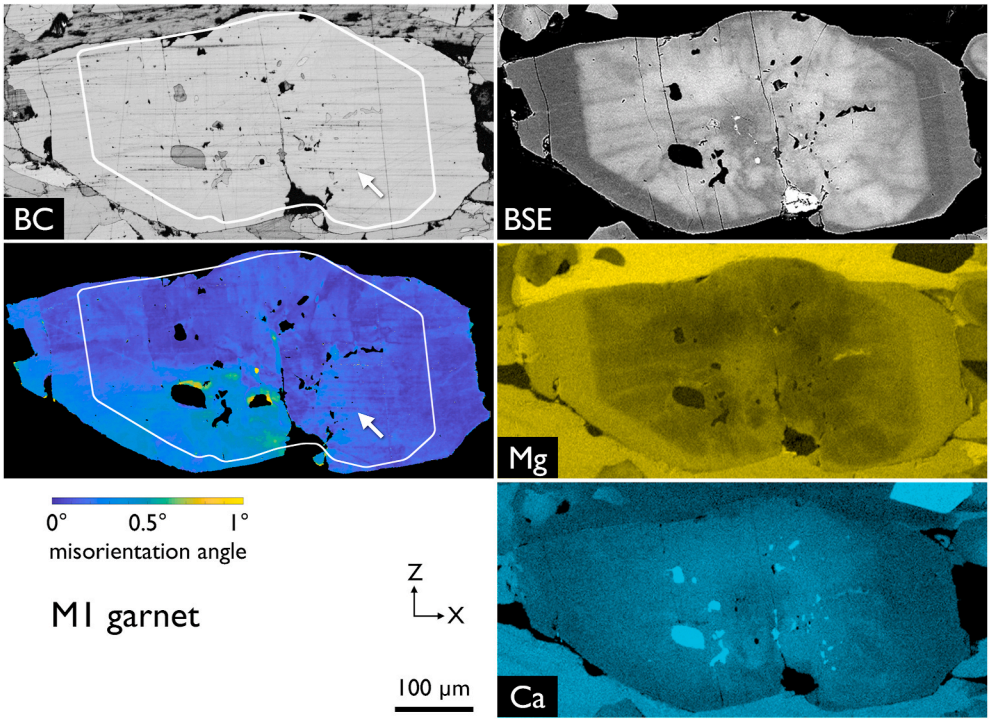

Fig. 4. Garnet zonation from a Bohemian massif eclogite.Left: Band contrast (BC) and misorientation map (showing angles of mis2mean) of a garnet grain from sample M1 with boundary of zonation superposed. Note that misorientation angles are extremely small (<1°). Note also that misorientation boundaries may be induced by scratches (compare with BC, white arrows), but do not coincide with zonation boundaries. Right: Back scatter contrast image (BSE) and element maps (Mg = yellow, Ca = turquois). Note that the zonation spacing is widest parallel to the stretching direction X, but not truncated on faces normal to the shortening direction Z. (For interpretation of the references to color in this figure legend, the reader is referred to the Web version of this article)

towards a girdle distribution normal to lineation in sample M1. {100} is oriented in incomplete single girdles (normal to lineation) with a tendency towards a diffuse or elongated maximum near the center of the pole figure (in the foliation plane; Fig. 10). All of these fabrics can be described as LS-fabrics with some tendency towards L-fabrics in the sense of Helmstaedt et al. (1972) and Keppler (2018).

Garnets do not show a systematic distribution for poles to {100}, {110}, and {111}, and J-indices are very low (Fig. 10). Some local maxima in pole figures represent larger single grain orientations. The hornblende CPO in M6 and M7 is of a similar type as that of omphacite but with weaker and more distributed maxima of all measured reflections compared to omphacite (and lower J-indices except for M7; Fig. 10). The sample M1 shows a rather patchy and different distribution of the hornblende CPO from omphacite for {100}, {001}, and {010} poles. Patchy submaxima in the hornblende distribution represent orientations of single grains because of their large size, similar to garnet (Fig. 10). The CPO of Tauern Window eclogite EK-H is similar to those of the Bohemian massif ones with a slightly stronger tendency towards a girdle fabrics for {001} in omphacite (Fig. 10). Garnets also show a nearly random distribution. The CPO's of garnet are more patchy than those of the Bohemian samples. This feature may be caused their larger grain size.

Misorientation maps for single grains of garnet and omphacite were calculated from EBSD data. In all measured omphacite and garnet grains, the misorientation angle is less than 1° with respect to the mean orientation of the grain (Figs. 4, 7–9). The highest misorientation angles are usually observed along scratches induced by sample preparation (Figs. 7–9). The measurements confirm that the zoned grains are single crystals and no substantial change in crystal orientation occurs with chemical variation. As pointed out for the chemical zonation patterns, there are healed cracks that extend into the inner parts of garnet grains. Some of these cracks may produce very small angles between the healed fragments (<0.5°; Fig. 4). These cracks form after the growth of garnets.

3.4. Phase distribution in the Bohemian eclogites

The spatial distribution of the phases garnet, omphacite and quartz has been analyzed. The distributions of each of the three phases within the eclogite have been evaluated separately (Fig. 11a,c). From the frequencies of the grain and phase boundaries, a more or less random distribution may be inferred in sections M1 and M7 parallel to elongation, as can be seen from the fact that they all plot on or very close to the phase boundary curves for random spatial distributions (black line in Fig. 11 c). Perhaps for the garnet distribution in M1, a slight ordering could be inferred as it shows slightly more phase boundaries than expected for the random case (Fig. 11c). In Fig. 11 b, d, the spatial relations of pairs of phases are explored. It appears that in M1 and M7, omphacite and garnet are randomly mixed (phase boundary frequencies plot on the black line in Fig, 11 d). In contrast, garnet and quartz exhibit excess frequencies of phase boundaries implying that the distribution is highly ordered (Fig. 11 b, d). For quartz and garnet there is a close spatial association of these two phases shown from the dominance of quartz-garnet phase boundaries and lower-than-expected frequency of quartz and garnet grain boundaries (Fig. 11 d). In Fig. 11b, this close association of quartz and garnet is most pronounced in direction parallel to the lineation (strain shadows; Fig. 11b).

3.5. Shape fabrics of omphacite, garnet, and quartz in Bohemian Massif eclogites

For XZ sections the results of the SURFOR and ACF analyses all show a consistent alignment with the lineation (extension direction) and a trend of substantially greater aspect ratios for omphacite (~2.2–2.8) than for garnet (~1.4–1.55) and quartz (~1.55–1.8) as can be seen by comparing Fig. 2 and Fig, 12. If garnet and quartz are considered together (quartz often is located next to the garnet in the direction parallel to lineation), their combined aspect ratio from the ACF analysis is higher (~1.7–2.15) than that of garnet and quartz alone but still lower than that of omphacite (Fig. 12). Unfortunately, the phase maps acquired on the YZ sections are too small, i.e., they do not contain enough grains for a statistically sound analysis to consider the problem in 3 D. However, visual inspection of the phase distributions (Fig. 1) does not indicate any systematic neighborhood relationships or grain shapes for garnet and quartz in the section normal to lineation as it is found in the

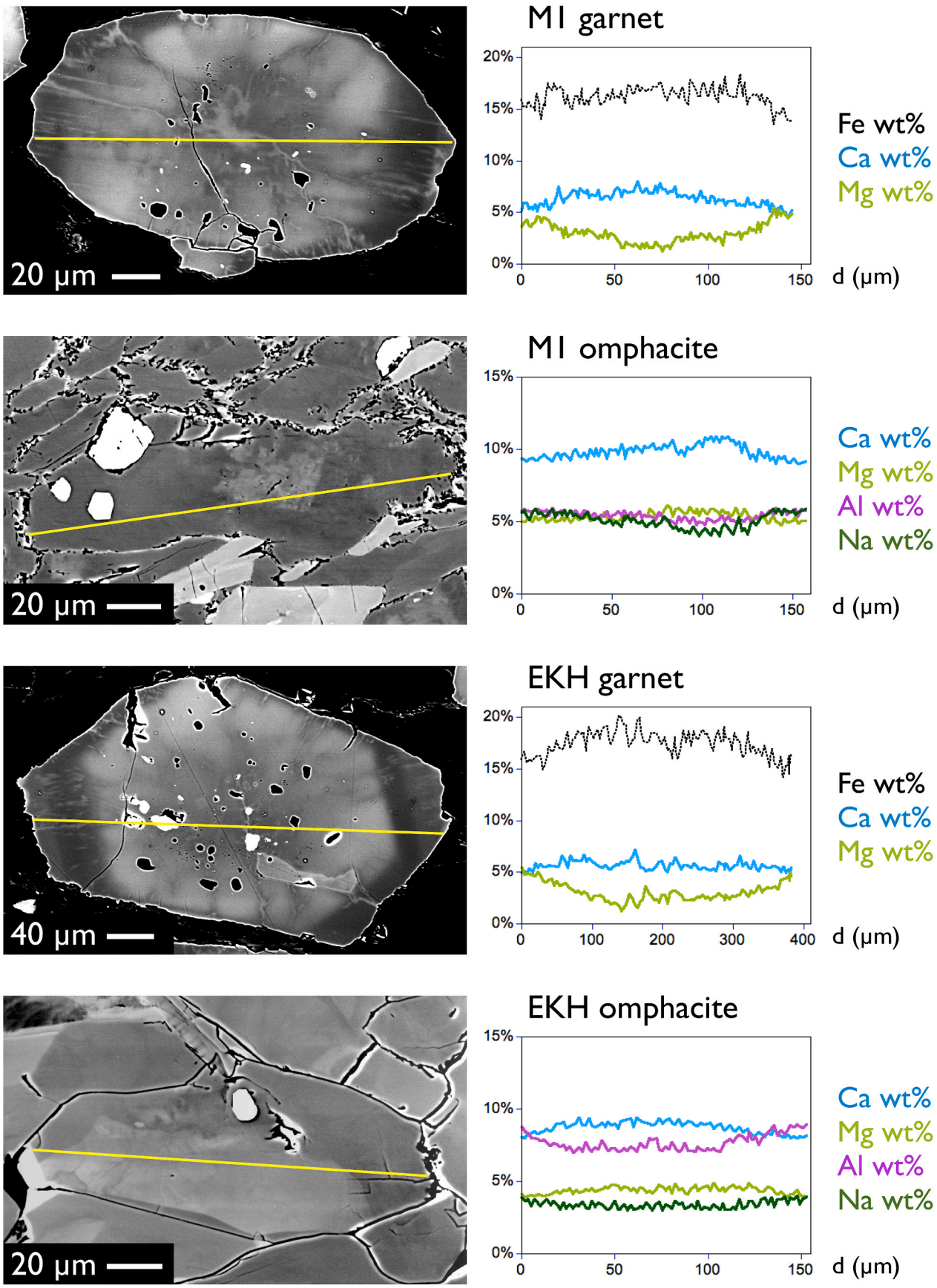

Fig. 5. Element concentration profiles for garnet and omphacite. Concentrations along profiles across garnet and omphacite grains from the Bohemian massif (M1) and the Tauern Window (EKH) eclogites are shown.

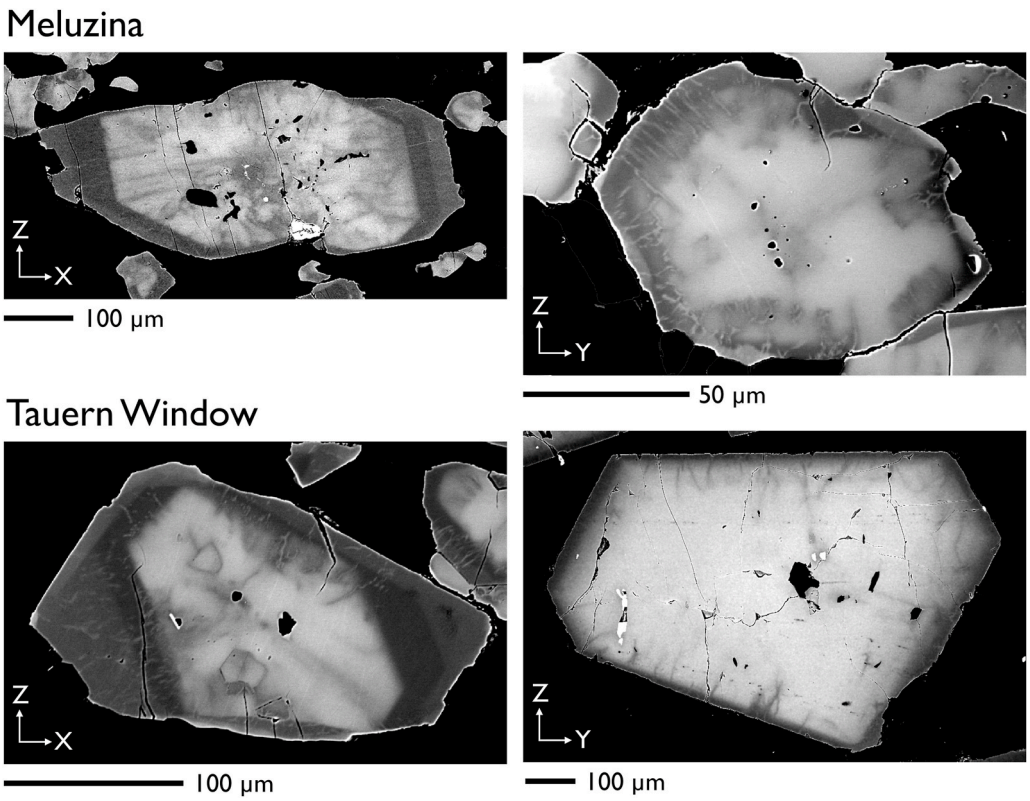

Fig. 6. Chemical zonation patterns parallel and normal to lineation in garnets from the Meluzina and Tauern sections. Left: XZ-sections, Right hand figures: YZ-sections. The YZ-sections show approximately the same thickness of growth rims around the cores in all directions.

section parallel to lineation, and fabrics appear rather isotropic.

4. Discussion

4.1. Compositional zonation in garnet and omphacite and their relationship to the P,T-development

The P,T-evolution of the Erzgebirge eclogites from the Meluzína locality has been studied in detail by Klápová et al. (1998) and Collett et al. (2017). Chemical compositions of garnet and omphacite in our samples are similar to the observations in those publications. Some of our samples (Fig. 7) concur with the conclusions of Collett et al. (2017), who reported an absence of systematic compositional variation in omphacite, but all of our observations (Fig. 5) show a compositional zoning. Thermodynamic modelling of the metamorphic evolution of the Meluzína locality eclogites by Collett et al. (2017) has confirmed that the observed chemical zonation in garnet is compatible with prograde garnet growth from P,T-conditions of ~500 °C and 1.9 GPa to the metamorphic peak at ~620 °C and 2.6 GPa. The same authors modelled the evolution of the jadeite content in omphacite along the same metamorphic path and predicted only subtle compositional variations. Our observations of the omphacite zonation also show subtle (~0.5–1 wt.%), but clearly developed and systematic increase in Na, and decrease in Ca content from core to rim accompanied by increase in Al content (Fig. 5), which we interpret primarily as an increase in the jadeite component of the omphacite during growth, possibly accompanied by a decrease in the aegirine component. Thus, both, garnet and some omphacite zonations in the Meluzína eclogites indicate growth of these minerals on a prograde pressure and temperature path consistent with increasing pressure during on-going subduction up to metamorphic peak conditions. This prograde path is shown in Fig. 13 marked with „prograde growth“ for omphacite and garnet.

Zoisite is the most elongated mineral phase in the assemblage. As zoisite is a dense hydrous phase, it is consistent with the P,T-path that it has formed during high pressure conditions. However, its stability field is so large that it is impossible to demonstrate that its formation occurred exclusively during the eclogite facies stage.

The hornblende grains overgrowing the fabric indicate amphibolite facies P,T conditions (Fig. 13), followed by the formation of thin symplectites of plagioclase and diopsidic pyroxene as rims on omphacites, inferred from microstructural relationships (Klápová et al. (1998); Collett et al. (2017)). Both assemblages indicate retrograde P,T conditions outside the eclogite facies. The random shape orientation of amphibole grains indicates a postkinematic growth, so that the deformation of these Bohemian eclogites has taken place only during prograde eclogite facies conditions. Formation of hornblendes and cpx-plag-symplectites is of limited extent in our samples, so that for the largest volume of the Meluzína eclogites preserves the high pressure P.T history and represents practically all of the deformation history.

The zonation pattern for garnet in the Tauern window eclogite shows a similar trend as that of the Bohemian eclogites, indicating garnet growth on a prograde (with respect to pressure) path. For omphacite, the zonation pattern is more oscillatory, so that the clear correlation with increasing pressure conditions is less clear. Thus, most fabrics analyzed in this study record synkinematic mineral reactions, and both sample series record at least a largest part of the deformation history of these rocks during high and possibly increasing pressure conditions.

The zonation pattern of garnet and omphacite in both sample series systematically follows the anisotropic shapes of these minerals produced during deformation, i.e. extension in the lineation direction. These microstructures indicate a direct correlation between deformation and the mineral growth of omphacite and garnet. It can be inferred that the deformation and mineral growth of garnet and omphacite have occurred simultaneously during the prograde mineral reaction.

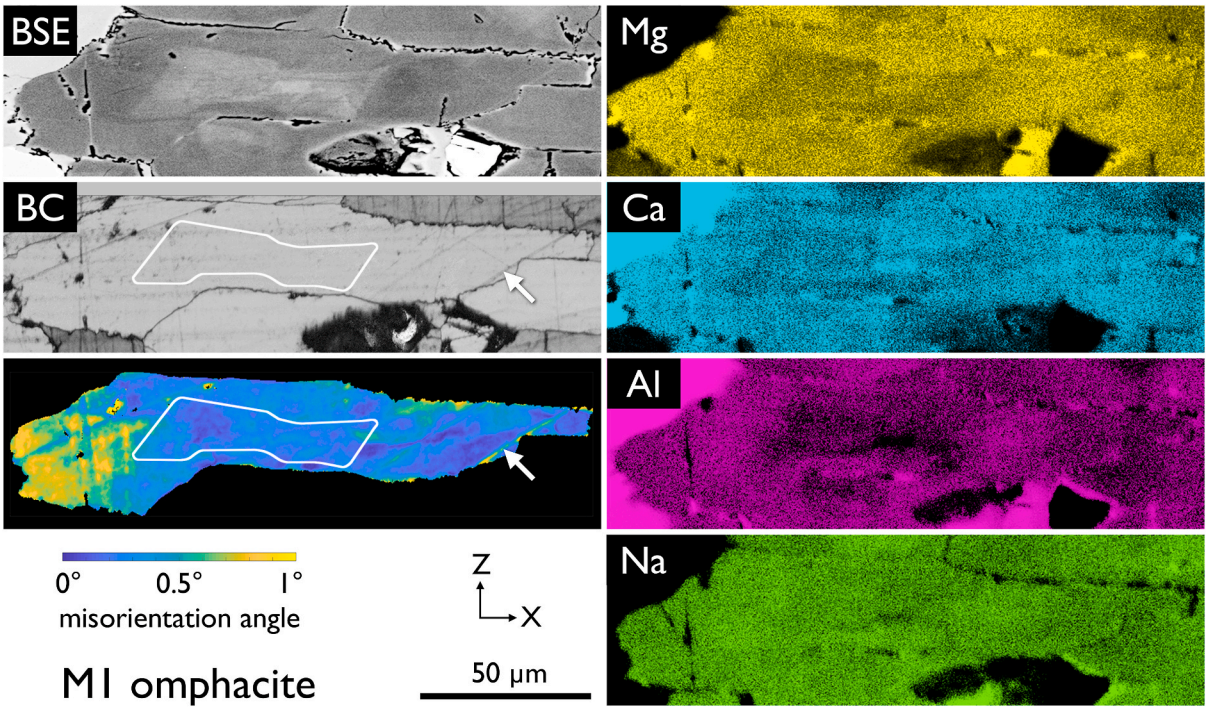

Fig. 7. Omphacite zonation from a Bohemian massif eclogite. Left: Back scatter contrast image (BSE), Band contrast (BC) and misorientation map (showing angles of mis2mean) of an omphacite grain from sample M1 with boundary of zonation superposed. Note that misorientation angles are extremely small (<1°). Note also that misorientation boundaries may be induced by scratches (compare with BC, white arrows), but do not coincide with zonation boundaries. Right: Element maps (Mg = yellow, Ca = turquois, Al = purple, Na = green). Note that the zonation is widest parallel to the stretching direction X and continuous on faces normal to the shortening direction Z. (For interpretation of the references to color in this figure legend, the reader is referred to the Web version of this article)

4.2. Processes of mineral growth and deformation

The concentric but anisotropically spaced zonation of the mineral composition can be traced outlining the grain shapes of garnet and omphacite usually without truncation in the outer parts of grains (Figs. 4–9). The lack of a truncation of the zonation patterns normal to the extension indicates that typically no dissolution has taken place. The outer parts of garnets, especially the faceted zonation patterns, represent growth zonations (Figs. 4, 5 and 8), and growth has occurred in *all* directions but at faster rates in the elongation direction and more slowly in the directions normal to it. The same interpretation can be made for omphacite grains (Figs. 5, 7 and 9), where growth anisotropy is more pronounced. Thus, there is no evidence for dissolution (e.g., pressure solution) in most garnet and omphacite grains in the direction normal to extension. Elongated garnet and omphacite grains are zoned from the cores to the rim with a consistent zonation pattern parallel and perpendicular to the rock's extension direction (Fig. 6).

Some inner parts of garnet show a more or less concentric but somewhat irregular zonation (Figs. 4 and 5), combined with healed cracks throughout the grains. These parts of garnet are best interpreted as a partial in-situ replacement of an existing garnet grain (e.g., Lanari and Engi, 2017; Giuntoli et al., 2018a). The cracks probably have formed during the replacement process and have acted as fluid pathways during the dissolution and reprecipitation of garnet, similar to processes described by Putnis (2009, 2015). The small misorientation of clasts in the grains' interiors can be explained by the cracking and healing processes (Fig. 4). However, these features are found throughout garnet grains cutting the growth zonations, so that they are later features.

The lack of dissolution indicates that the coupled processes of deformation and mineral growth during reaction have continued as long as there has been a reservoir of reactant phases (the original mafic assemblage of cpx and plagioclase), which have been consumed during the process. Growth in the extension direction has taken place only in the form of new phases. The clear connection between grain growth, anisotropic shape in garnets and omphacites, and their chemical zoning probably has for a large part developed during the prograde P,T evolution (Fig. 13) and corresponds to the progressive deformation of the Eclogites during on-going subduction.

4.3. Formation of crystallographic preferred orientation (CPO)

4.3.1. Omphacite and garnet

Omphacite CPO's form strong orthorhombic LS-type patterns with the normal to {001} parallel to lineation (Fig. 10). The dominant slip systems in omphacite have [001] and <110> Burgers vectors and prism {110} or {100} planes as glide planes (van Roermund and Boland, 1981; van Roermund, 1983; van Roermund, 1984, Buatier et al., 1991, Phillipot and van Roermnund, 1992; Godard and van Roermund, 1995). The [001]{110} slip system is common and known as pencil glide. Thus, a single [001] maximum in the lineation direction and {110} and {010} planes combined as maxima or girdle patterns normal to the lineation have been interpreted as an easy glide orientation of omphacite during deformation, and it is the reason why such omphacite CPO's are interpreted as evidence for dislocation creep deformation by many authors (van Roermund and Boland, 1981, van Roermund, 1983, van Roermund, 1984, Buatier et al., 1991, Phillipot and van Roermnund, 1992, Boundy et al., 1992, Godard and van Roermund, 1995, Abalos, 1997, Piepenbreier and Stöckhert, 2001, Mauler et al., 2001, Brenker et al., 2002, Bascou et al., 2002, Zhao et al., 2005, Zhang and Green, 2007, Rehman et al., 2016, Wassmann and Stöckhert, 2013). Kurz et al. (1998, 2004), Kurz (2005), Neufeld et al. (2008) and Keppler et al. (2015, 2016) studied eclogites from the Eclogite Zone (Tauern Window) to also conclude dislocation creep for these rocks. However, in the case of the Meluzína and Tauern Window eclogites analyzed here, the compositional growth zonation in elongated omphacite grains is not consistent with dominant dislocation glide or -creep deformation. The crystal misorientation in elongated omphacite grains is very small and identical in core and rim sections of the grains and independent of chemical

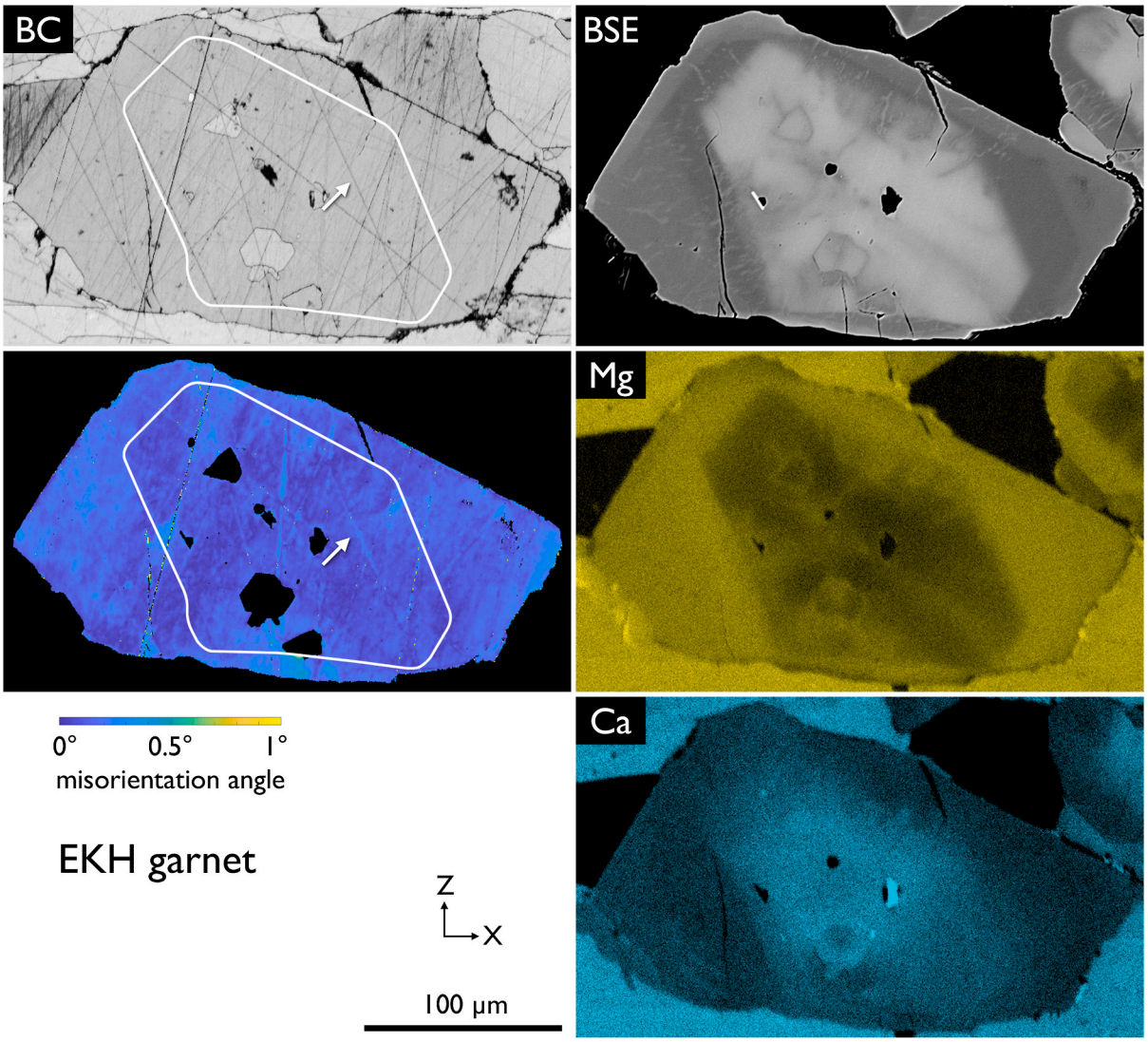

Fig. 8. Garnet zonation from a Tauern Window eclogite. Left: Band contrast (BC) and misorientation map (showing angles of mis2mean) of a large garnet grain from sample EKH with boundary of zonation superposed (small interior grains are not portrayed in misorientation map). Note that misorientation angles are extremely small (<1°). Note also that misorientation boundaries may be induced by scratches (compare with BC, white arrows), but do not coincide with zonation boundaries. Right: Back scatter contrast image (BSE) and element maps (Mg = yellow, Ca = turquois). Note that the zonation is widest parallel to the stretching direction X, but not truncated on faces normal to the shortening direction Z. (For interpretation of the references to color in this figure legend, the reader is referred to the Web version of this article)

composition (Figs. 7 and 9). This observation confirms that zoned omphacites are single crystals of up to a couple of hundred microns in length, and there is no evidence for dynamic recrystallization (neither subgrain rotation nor grain boundary migration), because no misorientation is detected. Instead, the observations and chemical data indicate only progressive anisotropic growth of elongated omphacite grains by faster rates in the extension direction during deformation. Such microstructures are indicative of grain scale diffusion creep rather dislocation creep deformation in these eclogites.

The difference between omphacite and garnet is that omphacite shows rather strong CPO's, whereas garnet does not show a significant CPO. This difference may be explained by anisotropic growth of omphacite that appears to be crystallographically controlled by surface energy (Hartman-Perdok-theory; Hartman and Perdok, 1955). The fastest growing planes in omphacite are (001), the slowest (010) (van Panhuys-Sigler and Hartman, 1981), i.e., the [001] direction usually is the fastest growth direction. If growth is controlled by deformation (e.g., the extension direction), a CPO of the observed type will result from growth ([001] parallel to lineation, (010) parallel to foliation), because suitably oriented nuclei grow faster than others. This mechanism for a formation of a CPO in omphacite has already been proposed by Godard and van Roermund (1995). For garnet as a cubic mineral, no crystallographically controlled shape anisotropy develops. Preferential growth occurs in the extension direction, but the growth direction is not crystallographically controlled (it is isotropic), so that any garnet crystal orientation can grow with anisotropic shapes.

The results of this study supporting diffusion creep as a dominant deformation mechanism partially agree and partially disagree with previous studies. Mauler et al. (2001) have argued that some of their CPO's of omphacite are produced by dissolution and precipitation (solution precipitation creep, which is considered as a type of diffusion creep), and Godard and van Roermund (1995), Phillipot and van Roermnund (1992), and Stöckhert (2002) have proposed subordinate diffusion creep deformation for Eclogites. While the results of our study support the precipitation (growth) part of diffusion creep, we see a complete zonation around all boundaries of the grains (no truncation perpendicular to the lineation), thus making dissolution of garnet and omphacite during deformation unlikely. The lack of solution features

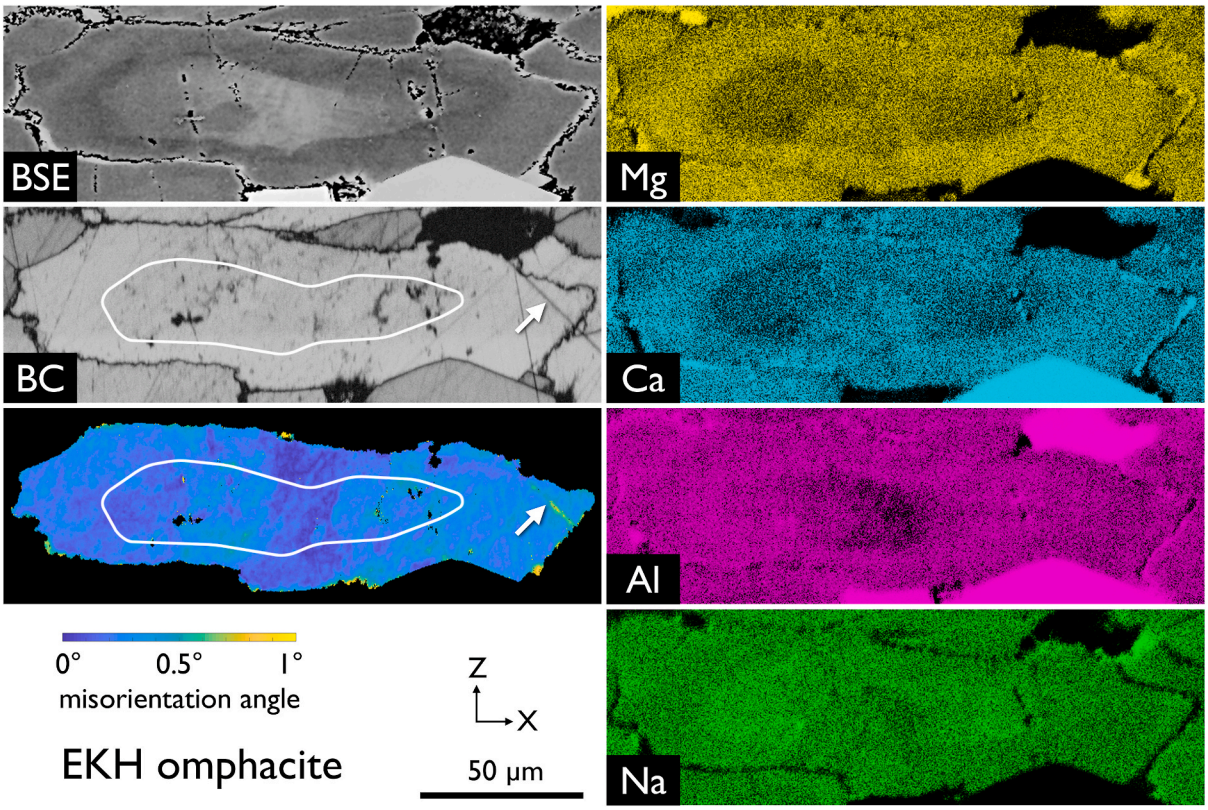

Fig. 9. Omphacite zonation from a Tauern Window eclogite. Left: Back scatter contrast image (BSE), Band contrast (BC) and misorientation map (showing angles of mis2mean) of an omphacite grain from sample EKH with boundary of zonation superposed. Note that misorientation angles are extremely small (<1°). Note also that misorientation boundaries may be induced by scratches (compare with BC, white arrows), but do not coincide with zonation boundaries. Right: Element maps (Mg = yellow, Ca = turquois, Al = purple, Na = green). Note that the zonation is widest parallel to the stretching direction X and continuous on faces normal to the shortening direction Z. (For interpretation of the references to color in this figure legend, the reader is referred to the Web version of this article)

indicates that the garnet and omphacite record primarily growth of these phases. The dissolution part of the diffusive mass transfer has taken place in form of dissolution of the reactant phases of the metastable assemblage during the metamorphic reaction. In this way, the diffusion creep deformation is directly connected to the metamorphic reaction as a part of the transformation process. While Mauler et al. (2001) focused only on omphacite, our study shows that garnet and omphacite both show chemical variations and geometries consistent with deformation and growth during the metamorphic evolution. For the zoisite, the same mechanism is inferred and probably has taken place simultaneously with growth of omphacite and garnet.

Some studies favor dislocation creep as the dominant deformation mechanism, based on clear evidence of dislocations and dislocation substructures from TEM observations (van Roermund, 1983; van Roermund, 1984, Buatier et al., 1991, Phillipot and van Roermnund, 1992; Müller and Franz, 2008, Müller et al., 2004, 2008). These TEM results are undisputed by our study, but it is one of the disadvantages of TEM studies that the statistical importance of the observed structures is difficult to assess because of the small size of the observed regions. It is quite possible that subordinate dislocation glide and/or creep may have occurred in our samples, too, but the microstructures clearly indicate that the dominant deformation mechanism is diffusion creep.

The hornblende CPO is similar to that of omphacite in Bohemian Massif and Tauern window eclogites (Fig. 10), but the fact that amphibole overgrows the fabric as a postkinematic phase indicates that deformation had ceased at the end of the reaction process (eclogite facies conditions) and new reactions (amphibolite facies overprint) took place under static, non-deformational, conditions (e.g, Fig. 13). Hornblende has primarily replaced omphacite during the amphibolite facies metamorphic reaction. Replacement of clinopyroxene by hornblende along planes with coherent interphase boundaries parallel to the [001] zone axis has been documented by Handy and Stünitz (2002). The observed hornblende CPO is inferred to be inherited from the preexisting omphacite CPO, i.e. hornblende grains nucleate with coherent boundaries on clinopyroxene and progressively replace omphacite with certain common crystal plane orientations.

4.4. Nucleation and growth of garnet, omphacite, and quartz

Spatially, garnet and omphacite are randomly distributed in the samples (Fig. 11). The distribution of phases is primarily controlled by nucleation during the metamorphic reaction (all minerals of the eclogite assemblage have nucleated as new phases – none of the original magmatic minerals have been preserved). The random spatial distribution of garnet and omphacite suggests homogeneous nucleation (i.e. random nucleation sites) for these phases. Garnet has a larger grain size than omphacite, possibly due to slower nucleation rates.

Absolute average length of garnet and omphacite in the extension direction is approximately the same, so total garnet growth in the extension direction may have been similar to that of omphacite. If grains are growing anisotropically and/or at different rates, a relative movement between them along their boundaries may become geometrically necessary. Such a movement takes place by (frictionless) grain boundary sliding (GBS) during diffusion creep deformation (Fig. 14) and is termed „Lifshitz sliding“ (e.g., Langdon, 2006). If, close to the completion of all mineral reactions, growing garnet and omphacite grains need to glide past each other in a random aggregate of phases, strain shadows may be formed around the more competent mineral garnet (Fig. 14c; this part of figure only shows the last stages of the growth and only the vicinity of garnet). Quartz is predominantly found next to garnet grains parallel to

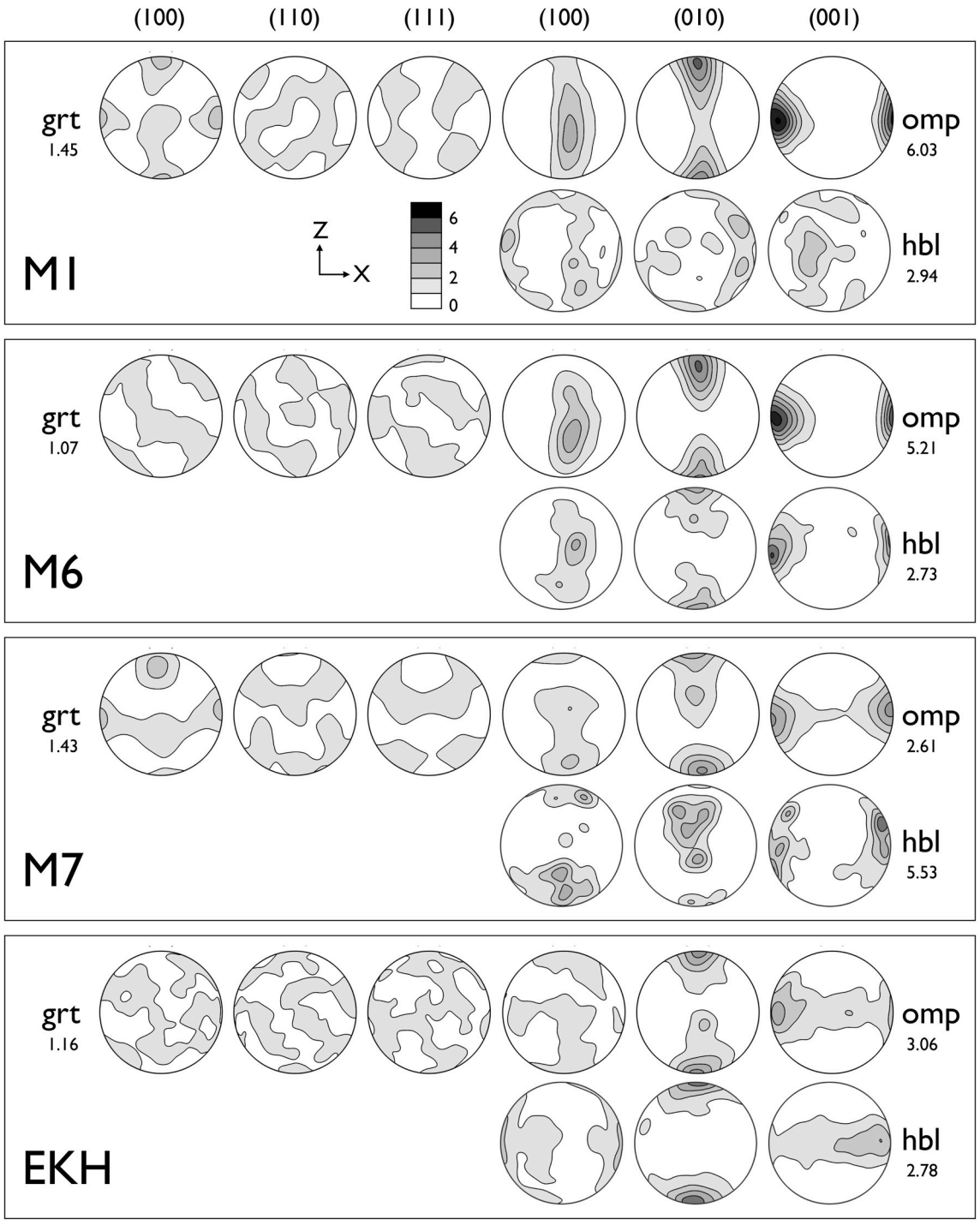

Fig. 10. Crystallographic preferred orientation (CPO) of garnet, omphacite, and hornblende from the Bohemian massif (M1, M6 and M7) and the Tauern Window (EKH) eclogites. Left: pole figures of (100), (110) and (111) of garnet; right, pole figures of (100), (010) and (001) of omphacite (above) and hornblende (below). Contours are multiples of the uniform distribution. J-indices are indicated below the mineral name.

the extension direction (Figs. 1, 11 and 12). It is inferred that the quartz has precipitated in the low stress sites of garnets as a consequence of local strain incompatibility (Fig. 14). This phenomenon may lead to a creep cavitation process (e.g., Kassner and Hayes, 2003; Fusseis et al., 2009) and has been observed in experiments and natural rocks (Rybacki et al., 2008; Menegon et al., 2015, Précigout and Stünitz, 2016). One important contributing factor for the precipitation of quartz is that the solubility of SiO_2 increases strongly and non-linearly with confining pressure (e.g., Manning, 1994, 2004, and references therein). Therefore, at eclogite facies conditions, a local lowering of the normal stress on a grain boundary surface normal to the extension direction will cause immediate oversaturation of the fluid with SiO_2 and will easily facilitate the nucleation and precipitation of quartz in these low stress sites (garnet strain shadows; Figs. 1, 12 and 14). In this way, deformation and mineral reaction/precipitation sites are directly connected via strain incompatibility/dilatancy and element solubility.

The shape fabrics, mineral zonations, and CPO's of omphacite and garnet in the analyzed Tauern Window eclogites are similar to those of the Meluzina eclogites and the deformation of omphacite and garnet during the proceeding metamorphic reaction is interpreted in the same

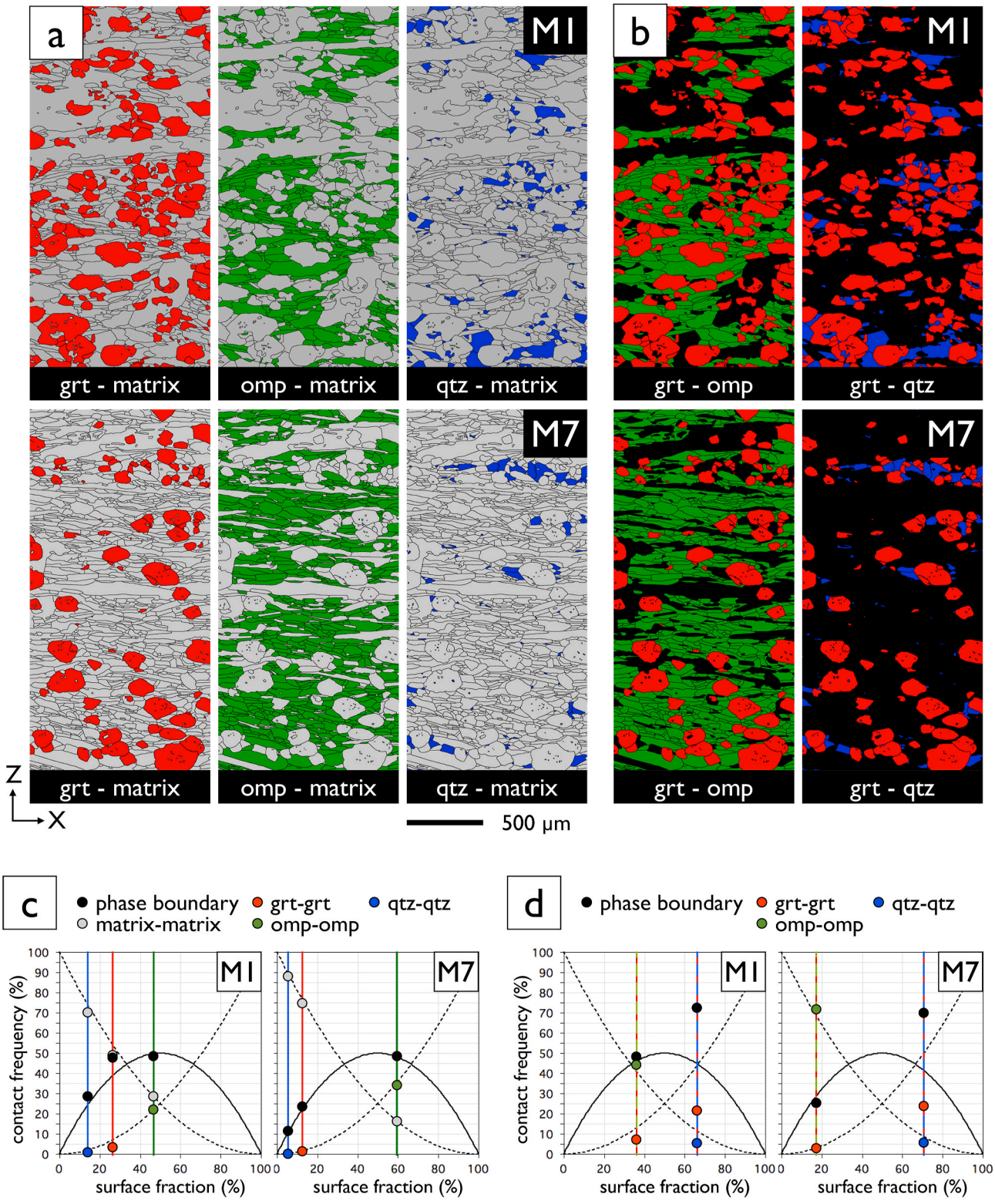

Fig. 11. Contact area analysis for samples from the Bohemian massif eclogite. Sections of samples M1 and M7 parallel to lineation are used. (a) Maps showing spatial distribution of garnet (grt, red), omphacite (omp, green) and quartz (qtz, blue) with respect to all other phases ('matrix', grey). (b) Analysis of only two phases: garnet versus omphacite (red-green) and garnet versus quartz (red-blue). The remaining phases (black) are not considered. (c) Plots of contact frequencies versus surface fractions for maps shown in (a). Note: The contact frequencies of the phase boundaries (black dots) and those of the grain boundaries (colored dots) plot on or close to the expected values for a random distribution (denoted by the solid and stippled curves, respectively) indicating that grt, omp and qtz are randomly distributed in the eclogite. (d) Plots of contact frequencies versus surface fractions for maps shown in (b). Note: The contact frequency of the phase boundaries (black dots) between grt and omp and the grt-grt and omp-omp grain boundaries plot on or close to the expected values for a random distribution (solid black and stippled curves, respectively), indicating that grt and omp are randomly distributed with respect to one another. In contrast, the phase boundaries for grt and qtz (black dots) plot high above the curve indicating a strong 'ordering' of grt and qtz. (For interpretation of the references to color in this figure legend, the reader is referred to the Web version of this article)

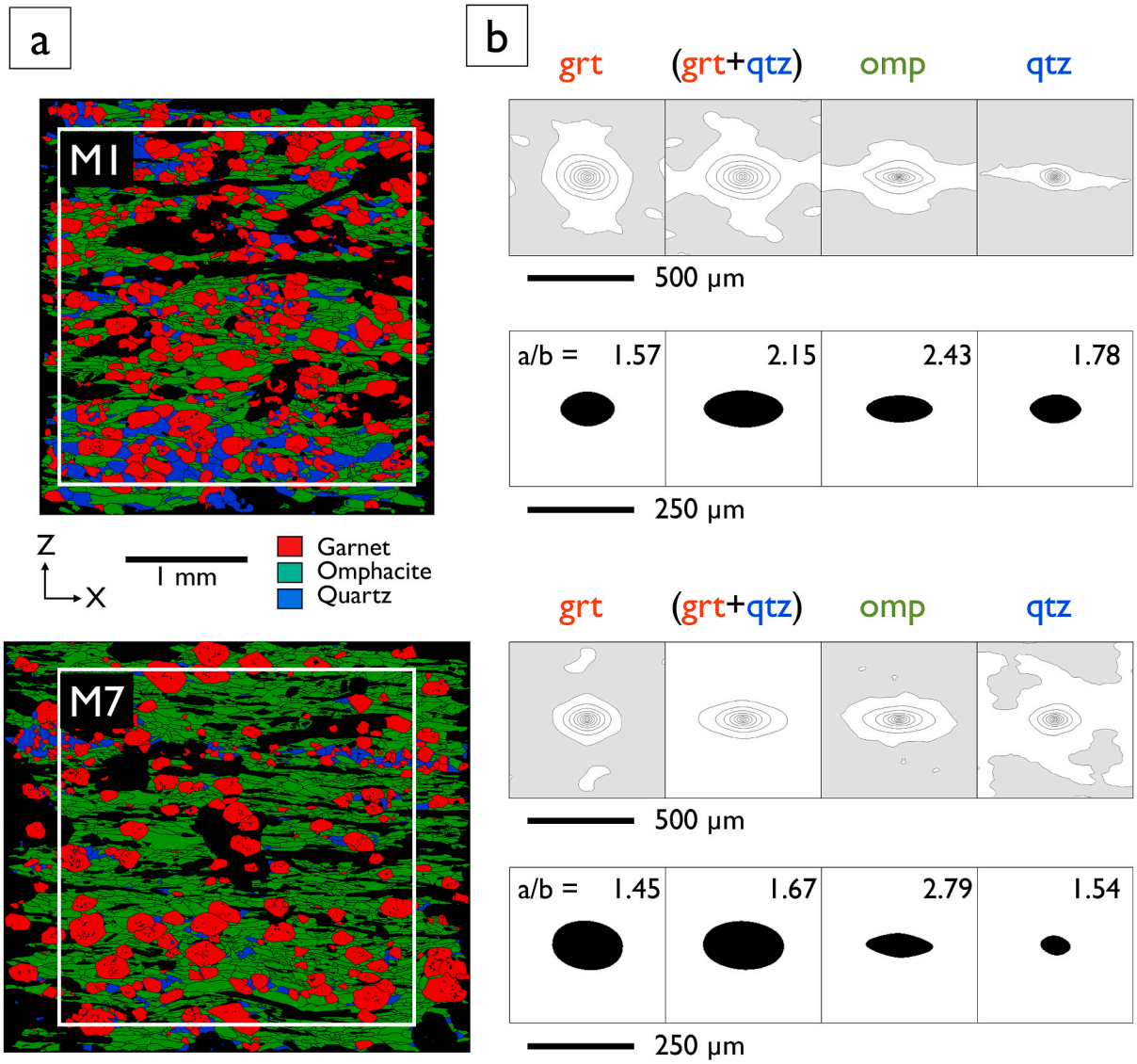

Fig. 12. Autocorrelation analysis of Bohemian massif eclogites. Separate autocorrelation functions (ACF) of garnet, omphacite, quartz and of garnet-quartz aggregates of samples M1 (top) and M7 (bottom), sections parallel to lineation. (a) Phase maps showing spatial distribution of garnet, omphacite and quartz; square shows area used for ACF analysis. (b) Top row: Magnified ACF centers, contours at 10% of ACF_{max}, <10% = grey. Bottom row: Magnified ACFs centers, thresholded at 39%, aspect ratio indicated.

way as in the Meluzina eclogites here, namely by diffusion creep and growth of the phases in the elongation direction. Quartz precipitating in garnet strain shadows show qualitatively the same characteristics and fabric distribution as in the Meluzina eclogites, too.

4.5. Shape fabrics (SPO) of omphacite and garnet

Previous studies of the Tauern Window eclogites (Kurz et al., 1998, 2004; Keppler et al., 2015, 2016) have suggested dislocation creep for the origin of these fabrics and they interpret the observed differences in SPO and CPO development as a function of strain state (constrictional, flattening), similar to Helmstaedt et al. (1972), as it is inferred by many previous studies (e.g., Bascou et al., 2002; Keppler, 2018, and references therein). The CPO's are discussed above, in this section we address the question of the SPO's.

The garnet and omphacite fabrics in the Meluzina Eclogites show distinct differences (Fig. 3): the garnet shapes plot near the k = 1 line in the Flinn fabric diagram, whereas the omphacites plot clearly in the uniaxial elongation fabric field. The interpretation of diffusion creep and anisotropic growth of minerals made here can explain the observed difference between garnet and omphacite shapes: Omphacite has only one preferred growth direction ([001]). If growth takes place preferentially in this direction, the resulting shapes will be rods, or slightly triaxial rods for the case of (010) being the most slowly growing crystal face (van Panhuys-Sigler and Hartman, 1981). If rods are forming as a consequence of elongation in a single direction during growth, the plane strain and the constriction states of strain cannot be distinguished well, because in both cases, fastest growth occurs in the elongation direction, regardless of the shortening directions (only in the case of pronounced triaxial shapes with (010) as larger crystal faces could the shapes be distinguished and/or in the case of dissolution in the shortening direction). Only a flattening state of strain is expected to form rods in many different directions within the foliation plane during growth, because there is more than one extension direction. The SPO and CPO are connected for omphacite. Thus, for omphacite, the resulting SPO will always be "constrictional" in both, simple shear and constrictional deformation. Garnet as a phase without a preferential crystal growth direction might be better for inferring a strain state from the SPO. The difference between the garnet and omphacite SPO's in the Meluzina case (Figs. 2 and 3) may be reconciled by proposing a plane strain

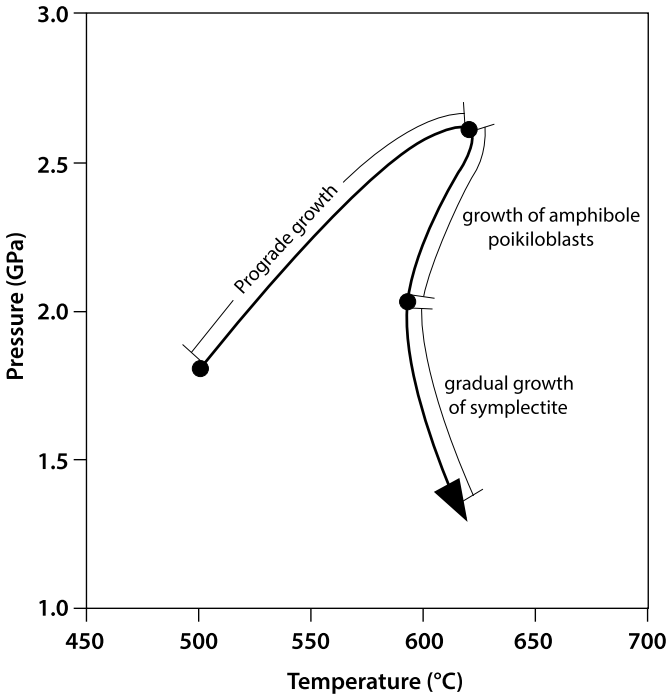

Fig. 13. P,T-path of the Bohemian eclogites. P,T-path as compiled from Klapová et al. (1998) and Collett et al. (2017). Some of the zonations of omphacite and garnet in the analyzed samples indicate a formation of the eclogite assemblage during the prograde path.

deformation state, where garnet may grow according to the strain state while omphacite grows only in the elongation direction, producing rod-like SPO's because of crystallographically controlled growth kinetics. The situation illustrates that even though in grain scale diffusion creep the grain shapes may bear some qualitative indication about strain, the shape fabrics cannot be used to calculate finite strain, because growth anisotropy, rates, grain boundary sliding, etc. will control finite grain shapes.

4.6. Polymineralic deformation and application to deformation processes

The CPO's and elongated grain shapes of omphacite are rather common for eclogites, so that it is likely that similar CPO's and SPO's in other eclogites could also be the result of diffusion creep deformation rather than dislocation creep. This situation would be consistent with the conclusion by Piepenbreier and Stöckhert (2001), who argued that dislocation creep is the exception rather than the rule in eclogite facies rocks. Their conclusion is partly based on the fact that inferred stresses in subduction zones are low (Stöckhert, 2002; Stöckhert and Renner, 1998; Gerya and Stöckhert, 2002; Wassmann and Stöckhert, 2013), and dislocation creep laws of diopside and omphacite (both belong to the same isomechanical group; Dorner and Stöckhert, 2004) yield flow stresses that seem to be unrealistically high at geological strain rates (Dimanov et al., 2003, 2007; Dimanov and Dresen, 2005; Orzol et al., 2003; Zhang et al., 2006; Moghadam et al., 2010). The latter study infers differential stresses of up to 1 GPa for omphacite dislocation creep deformation for typical eclogite facies temperatures of 550–700 °C (Moghadam et al., 2010).

One of reasons why dislocation creep dominates in experiments of omphacite (Zhang et al., 2006) may be that omphacite is deformed as a single phase material and the high stresses applied in these experiments force dislocation creep to operate, because no chemical reaction can occur. The eclogite deformation studied here takes place (a) in a polyphase rock rather than a monophase material and (b) *during* the omphacite and garnet forming reaction, i.e. during the metastability of

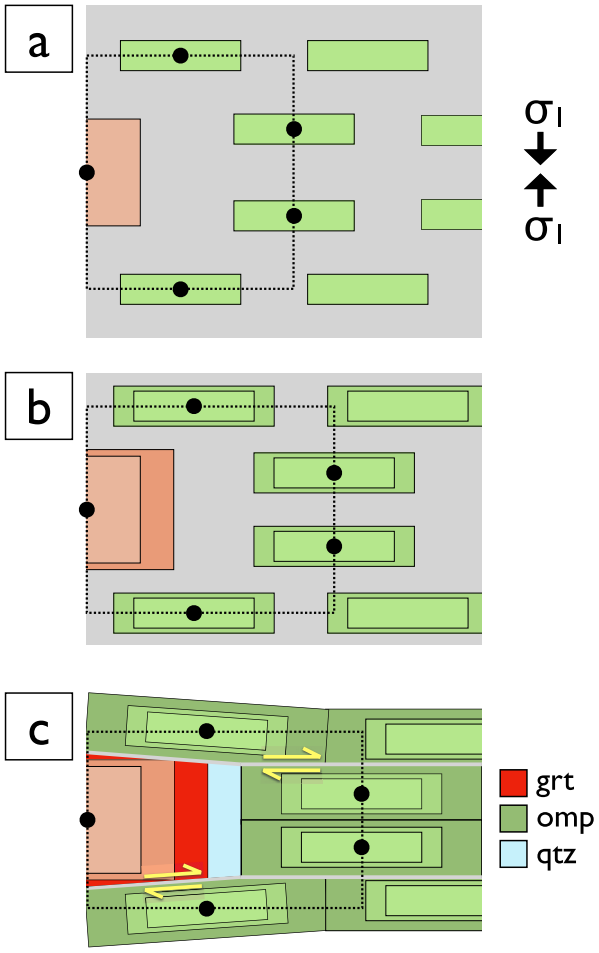

Fig. 14. Schematic drawing of deformation of mafic rock undergoing phase transformation to eclogite.(a) Near the beginning of deformation (σ_1-direction indicated); nucleation of garnet and omphacite in deforming parent rock (mafic rock, grey matrix). Centers of nucleation (black dots) act as passive markers of the matrix deformation, as outlined by stippled rectangles. (b) Consumption of reactants (grey) and growth of products, garnet and omphacite, parallel to extension. Note: garnet grains grow from equant to elongated shapes (growth rate is independent of crystallographic orientation of nucleus), omphacite grains are elongated from the start (growth rates are controlled by crystallography). (c) Phase transformation near completion: Garnet and omphacite form local load bearing networks. Lifshitz grain boundary sliding may take place at all grain boundaries where growth, i.e., mineral reactions are still ongoing (two sites indicated by yellow arrows). Quartz precipitates in the low stress sites where the growth rates of garnet and omphacite lag behind the bulk extension rate. Once all reactions are completed, deformation of eclogite ends, i.e., cannot continue at the given stress level. (For interpretation of the references to color in this figure legend, the reader is referred to the Web version of this article)

the pre-existing reactant phases plagioclase and pyroxene. It is inferred that the zonation in omphacite and garnet in the Meluzina eclogites developed over a range of P,T-conditions and while a reservoir of reacting phases had still been present (and dissolving while omphacite and garnet precipitate and grow). In such a case, the diffusion creep deformation is part of a transformation process (metamorphic reaction). Experimental testing of a single phase (omphacite) within its P, T-stability field does not allow for chemical driving potentials to play a role in the deformation. Metastability of phases during deformation has been shown to be important for mechanical weakening in nature (e.g., Hidas et al., 2013) and in experiments (Stünitz and Tullis, 2001; de Ronde et al., 2004, 2005; Holyoke and Tullis 2006a, b; Marti et al., 2017, 2018, Mansard et al., 2020) and in nature (e.g., Handy and Stünitz,

2002; Menegon et al., 2013; Okudaira et al., 2015), promoting diffusion creep. Thus, dislocation creep may be a forced mechanism in deformation experiments of the stable monophase material, while diffusion creep may be dominant in nature due to metastability of the phases in a polymineralic rock. The metastability of phases in a polymineralic assemblage emphasizes the importance of transformation processes during deformation in polyphase materials.

The CPO, SPO, and compositional zonations of omphacite indicate that nucleation and preferential growth of phases can produce a strong CPO during diffusion creep deformation, and that well developed CPO's are not necessarily the product of dislocation creep. Similar results have been presented by Misch (1969), Berger and Stünitz (1996), Getsinger et al. (2013), Getsinger and Hirth (2014), and Giuntoli et al. (2018b) for amphiboles (natural samples and experiments) and by Sundberg and Cooper (2008) for harzburgite (experiments) and Barreiro et al. (2007) for plagioclase (experiments). The preferred nucleation of quartz at low stress surfaces of garnet during creep cavitation in diffusion creep is a consequence of strain incompatibility between garnet and faster growing (deforming) omphacite.

The processes described here constitute the direct connection between mineral reactions and deformation and may represent an important if not typical deformation situation in polymineralic rocks. The example of eclogite indicates that mafic rocks can become mechanically weak *during* the general transformation process (transformation weakening), i.e. the interaction of mineral reaction and deformation by diffusion creep. Despite the high strength of individual phases (pyroxenes, garnet, zoisite) in dislocation creep, mafic rocks undergoing a transformation may deform by diffusion creep, which typically implies n-values ≈ 1, consistent with low stresses. This is particularly important in mafic rocks, which consist of mechanically strong phases (pyroxenes, amphiboles, plagioclase). The results are important for subduction zones in general and support the fact that in subduction zones, stresses are expected to be low as already demonstrated by Stöckhert (2002) and Stöckhert and Renner (1998). An exception are dry basement rocks that become incorporated in subduction zones. It is argued here that in addition, many initially strong lithologies (such as, e.g., dry basement rocks) can become weak, provided that reactions can proceed during deformation.

Diffusion creep is a grain size dependent deformation mechanism. The observed grain growth of phases during the metamorphic reaction will make diffusion creep deformation progressively less efficient. The transient nature of the deformation mechanism is given by two factors: (1) When the metamorphic reaction is complete, the weakening stops, and (2) grain growth makes diffusion creep less efficient.

5. Conclusions

Our study of two different eclogite units demonstrates that anisotropic crystal growth can produce eclogite deformation fabrics during progressive mineral reactions during subduction. Crystal plastic deformation (dislocation creep) is not identified as the dominant deformation mechanism as indicated by garnet and omphacite chemical growth zonation in single omphacite and garnet grains. The anisotropic grain shapes of omphacite are interpreted to have formed by preferential growth of grains in the [001] direction in the elongation direction during deformation. The resulting omphacite crystallographic preferred orientation (CPO) has developed as a consequence of anisotropic differential crystal growth and coincides with the mineral shape preferred orientation (SPO). Garnets form a random CPO. Their anisotropic shapes are also produced by anisotropic grain growth, but Garnet does not show a preferred crystallographic growth direction and therefore does not develop a CPO. The metastable reactants of the mafic assemblage are being dissolved and eclogite facies products precipitated producing a preferential growth fabric of minerals in the two analyzed sample series. The dissolution and precipitation of minerals constitutes a diffusion creep deformation (or solution transfer creep or dissolution precipitation creep - all of these terms describe very similar processes), for which typically low stress exponents are expected ($n \approx 1$). This transformation process weakens the rock and allows a deformation of mafic rocks at far lower stresses than those normally required by dislocation creep of pyroxenes and garnet. It is suggested that the transformation process itself is an important weakening mechanism in mafic (and other) rocks, facilitating deformation at low differential stresses.

Declaration of competing interest

The authors declare that they have no known competing financial interests or personal relationships that could have appeared to influence the work reported in this paper.

Acknowledgements

We thank Rüdiger Kilian for his help with MTEX calculations. Discussions with Pierre Lanari, Claudia Trepmann, Sumit Chakraborti, John Wheeler, Patrick Cordier, Jörg Renner, and Alfons Berger have helped to clarify some ideas. James Mackenzie has made the initial important observations in the Meluzina eclogites that have initiated this study. We are also indebted to careful reviews by Luca Menegon and an anonymous reviewer.

References

Abalos, B., 1997. Omphacite fabric variation in the Cabo Ortegal eclogite (NW Spain): relationship with strain symmetry during high-pressure deformation. Journal of Structural Geology 19, 621–637.
Abalos, B., Puelles, P., Gil Ibarguchi, J.I., 2003. Structural assemblage of high-pressure mantle and crustal rocks in a subduction channel (Cabo Ortegal, NW Spain). Tectonics 22, 1006–1127.
Agard, P., Yamato, P., Soret, M., Prigent, C., Guillot, S., Plunder, A., Dubacq, B., Chauvet, A., Monié, P., 2016. Plate interface rheological switches during subduction infancy: control on slab penetration and metamorphic sole formation. Earth Planet Sci. Lett. 451, 208–220.
Agard, P., Plunder, A., Angiboust, S., Bonnet, G., Ruh, J., 2018. The subduction plate interface: rock record and mechanical coupling (from long to short time scales). Lithos 320–321, 537–561.
Barreiro, J.G., Lonardelli, I., Wenk, H.R., Dresen, G., Rybacki, E., Ren, Y., Tomé, C.N., 2007. Preferred orientation of anorthite deformed experimentally in Newtonian creep. Earth Planet Sci. Lett. 264 (1–2), 188–207.
Bascou, J., Guilhem, B., Vaucez, A., Mainprice, D., EgydioSilva, M., 2001. EBSD-measured lattice preferred orientations and seismic properties of eclogites. Tectonophysics 342, 61–80.
Bascou, J., Tommasi, A., Mainprice, D., 2002. Plastic deformation and development of clinopyroxene lattice preferred orientations in eclogites. J. Struct. Geol. 24, 1357–1368.
Berger, A., Stünitz, H., 1996. Deformation mechanisms and reaction of hornblende: examples from the Bergell tonalite (Central Alps). Tectonophysics 257, 149–174.
Bons, P.D., den Brok, B., 2000. Crystallographic preferred orientation development by dissolution-precipitation creep. J. Struct. Geol. 22, 1713–1722.
Boundy, T.M., Fountain, D.M., Austrheim, H., 1992. Structural development and petrofabrics of eclogite facies shear zones, Bergen Arcs, western Norway: implications for deep crustal deformational processes. J. Metamorph. Geol. 10 (2), 127–146.
Brenker, F.E., Prior, D.J., Müller, W.F., 2002. Cation ordering in omphacite and effect on deformation mechanisms and lattice preferred orientation (LPO). J. Struct. Geol. 24, 1991–2005.
Buatier, M.V., Van Roermund, H.L.M., Drury, M.R., Lardeaux, J.T., 1991. Deformation and recrystallization mechanisms in naturally deformed omphacites from the Sesia-Lanzo zone; geophysical consequences. Tectonophysics 195 (1), 11–27.
Collett, P., Štípská, P., Kusbach, V., Schulmann, K., Marciniak, G., 2017. Dynamics of Saxothuringian subduction channel/wedge constrained by phase-equilibria modelling and micro-fabric analysis. J. Metamorph. Geol. 35, 253–280.
de Ronde, A.A., Heilbronner, R., Stünitz, H., Tullis, J., 2004. Spatial correlation of deformation and mineral reaction in experimentally deformed plagioclase–olivine aggregates. Tectonophysics 389 (1–2), 93–109.
de Ronde, A.A., Stünitz, H., Tullis, J., Heilbronner, R., 2005. Reaction-induced weakening of plagioclase–olivine composites. Tectonophysics 409 (1–4), 85–106.
Dimanov, A., Dresen, G., 2005. Rheology of synthetic anorthite-diopside aggregates: implications for ductile shear zones. J. Geophys. Res.: Solid Earth 110 (B7).
Dimanov, A., Lavie, M.P., Dresen, G., Ingrin, J., Jaoul, O., 2003. Creep of polycrystalline anorthite and diopside. J. Geophys. Res.: Solid Earth 108 (B1).
Dimanov, A., Rybacki, E., Wirth, R., Dresen, G., 2007. Creep and strain-dependent microstructures of synthetic anorthite–diopside aggregates. J. Struct. Geol. 29 (6), 1049–1069.

Dorner, D., Stöckhert, B., 2004. Plastic flow strength of jadeite and diopside investigated by microindentation hardness tests. Tectonophysics 379 (1–4), 227–238.
Finstad, A.K., 2017. Connection between Chemical Zonation and Crystallographic Preferred Orientation as an Indicator for the Fabric Development in Eclogites. MSc thesis. The Arctic University, Tromsø.
Franke, W., 2000. The mid-European segment of the Variscides: tectonostratigraphic units, terrane boundaries and plate tectonic evolution. In: Franke, W., Haak, V., Oncken, O., Tanner, D. (Eds.), Orogenic Processes, Quantification and Modelling in the Variscan Belt, vol. 179. Geological Society of London, Special Publications, pp. 35–61.
Fusseis, F., Regenauer-Lieb, K., Liu, J., Hough, R.M., De Carlo, F., 2009. Creep cavitation can establish a dynamic granular fluid pump in ductile shear zones. Nature 459 (7249), 974.
Gerya, T.V., Stöckhert, B., 2002. Exhumation rates of high pressure metamorphic rocks in subduction channels: the effect of rheology. Geophys. Res. Lett. 29 (8), 102-1.
Getsinger, A.J., Hirth, G., 2014. Amphibole fabric formation during diffusion creep and the rheology of shear zones. Geology 42 (6), 535–538.
Getsinger, A.J., Hirth, G., Stünitz, H., Goergen, E.T., 2013. Influence of water on rheology and strain localization in the lower continental crust. G-cubed 14 (7), 2247–2264.
Giuntoli, F., Lanari, P., Engi, M., 2018a. Deeply subducted continental fragments - Part 1: fracturing, dissolution-precipitation, and diffusion processes recorded by garnet textures in the Central Sesia Zone. Solid Earth 9, 167–189.
Giuntoli, F., Menegon, L., Warren, C.J., 2018b. Replacement reactions and deformation by dissolution and precipitation processes in amphibolites. J. Metamorph. Geol. 36 (9), 1263–1286.
Glodny, J., Ring, U., Kühn, A., Gleissner, P., 2005. Crystallization and very rapid exhumation of the youngest Alpine eclogites (Tauern Window, Eastern Alps) from Rb/Sr mineral assemblage analysis. Contrib. Mineral. Petrol. 149, 699–712.
Godard, G., van Roermund, H.L.M., 1995. Deformation-induced clinopyroxene from eclogites. J. Struct. Geol. 17, 1425–1443.
Gomberg, J., Cascadia, Beyond Working Group, 2007. Slow-slip phenomena in Cascadia from 2007 and beyond: a review. Bulletin 122 (7–8), 963–978, 2010.
Handy, M.R., Stünitz, H., 2002. Strain localization by fracturing and reaction weakening—a mechanism for initiating exhumation of subcontinental mantle beneath rifted margins. Geol Soc London, Special Publ 200 (1), 387–407.
Hartman, P., Perdok, W.G., 1955. On the relations between structure and morphology of crystals. I. *Acta Crystallographica* 8 (1), 49–52.
Heilbronner, R., Barrett, S., 2014. Image Analysis in Earth Sciences: Microstructures and Textures of Earth Materials. Springer Berlin Heidelberg.
Helmstaedt, H., Anderson, O.L., Gavasci, A.T., 1972. Petrofabric studies of eclogite, spinel-websterite and spinel lherzolite xenoliths from kimberlite-bearing breccia pipes in southeastern Utah and northeastern Arizona. J. Geophys. Res. 77, 4350–4365.
Hidas, K., Garrido, C., Tommasi, A., Padron-Navarta, J.A., Thielmann, M., Konc, Z., Frets, E., Marchesi, C., 2013. Strain localization in pyroxenite by reaction-enhanced softening in the shallow subcontinental lithospheric mantle. J. Petrol. 1997–2031. https://doi.org/10.1093/petrology/egt039.
Hielscher, R., Schaeben, H., 2008. A novel pole figure inversion method: specification of the MTEX algorithm. J. Appl. Crystallogr. 41, 1024e1037.
Holyoke, C.W., Tullis, J., 2006a. The interaction between reaction and deformation: an experimental study using a biotite+ plagioclase+ quartz gneiss. J. Metamorph. Geol. 24 (8), 743–762.
Holyoke, C.W., Tullis, J., 2006b. Formation and maintenance of shear zones. Geology 34 (2), 105–108.
Hoschek, G., 2001. Thermobarometry of metasediments and metabasites form the eclogite zone of the tauern window, eastern Alps, Austria. Lithos 59, 127–150.
Hoschek, G., 2007. Metamorphic peak conditions in the Tauern Window, Eastern Alps, Austria: thermobarometry of the assemblage garnet+omphacite+phengite+quartz. Lithos 93, 1–16.
Hoth, K., Lorenz, W., Berger, H., 1983. Die Lithostratigraphie des Proterozoikums im Erzgebirge. Z. Angew. Geol. 29, 413–418.
Hyndman, R.D., Yamano, M., Oleskevich, D.A., 1997. The seismogenic zone of subduction thrust faults. Isl. Arc 6 (3), 244–260.
Jeřábek, P., Konopásek, J., Žáčková, E., 2016. Two-stage exhumation of subducted Saxothuringian continental crust records underplating in the subduction channel and collisional forced folding (Krkonoše-Jizera Mts., Bohemian Massif). J. Struct. Geol. 89, 214–229.
Kassner, M.E., Hayes, T.A., 2003. Creep cavitation in metals. Int. J. Plast. 19 (10), 1715–1748.
Keppler, R., 2018. Crystallographic preferred orientations in Eclogites – a review. J. Struct. Geol. 115, 284–296.
Keppler, R., Ullemeyer, K., Behrmann, J.H., Stipp, M., Kurzawski, R.M., Lokajicek, T., 2015. Crystallographic preferred orientations of exhumed subduction channel rocks from the Eclogite Zone of the Tauern Window (Eastern Alps, Austria) and implications on rock elastic anisotropies at great depths. Tectonophysics 647–648, 89–104.
Keppler, R., Stipp, M., Behrmann, J.H., Ullemeyer, K., Heidelbach, F., 2016. Deformation inside a paleosubduction channel – insights from microstructures and crystallographic preferred orientations of eclogites and metasediments from the Tauern Window, Austria. J. Struct. Geol. 82, 60–79.
Klápová, H., Konopásek, J., Schulmann, K., 1998. Eclogites from the Czech part of the Erzgebirge: multi-stage metamorphic and structural evolution. J Geol Soc London 155, 567–583.
Kleinschrodt, R., McGrew, A., 2000. Garnet plasticity in the lower continental crust: implications for deformation mechanisms based on microstructures and SEM-electron channeling pattern analysis. J. Struct. Geol. 22 (6), 795–809.
Konopásek, J., 1998. Formation and destabilization of the high pressure assemblage garnet-phengite-paragonite (Krušné hory Mountains, Bohemian Massif): the significance of the Tschermak substitution in the metamorphism of pelitic rocks. Lithos 42, 269–284.
Konopásek, J., 2001. Eclogitic micaschists in the central part of the krušné hory Mountains (bohemian massif). Eur. J. Mineral 13, 87–100.
Konopásek, J., Schulmann, K., 2005. Contrasting Early Carboniferous field geotherms: evidence for accretion of a thickened orogenic root and subducted Saxothuringian crust (Central European Variscides). J Geol Soc London 162/3, 463–470.
Kossmat, F., 1927. Gliederung des varistischen Gebirgsbaues. In: Abhandlungen des Sächischen Geologischen Landesamtes, vol. 1.
Kotková, J., 1993. Tectonometamorphic history of lower crust in the Bohemian Massif – example of north Bohemian granulites. In: Czech Geological Survey Special Paper, vol. 2, pp. 56–97.
Kotková, J., O'Brien, P., Ziemann, M., 2011. Diamond and coesite discovered in Saxony-type granulite: solution to the Variscan garnet peridotite enigma. Geology 39, 667–670.
Kurz, W., 2005. Constriction during exhumation: evidence from eclogite microstructures. Geology 33, 37–40.
Kurz, W., Neubauer, F., Dachs, E., 1998. Eclogite meso- and microfabrics: implications for the burial and exhumation history of eclogites in the Tauern Window (Eastern Alps) from P-T-d paths. Tectonophysics 285, 183–209.
Kurz, W., Jansen, E., Hundenborn, R., Pleuger, J., Schäfer, W., Unzog, W., 2004. Microstructures and crystallographic preferred orientations of omphacite in alpine eclogites: implications for the exhumation of (ultra-) high–pressure units. J. Geodyn. 37, 1–55.
Lanari, P., Engi, M., 2017. Local bulk composition effects on metamorphic mineral assemblages. Rev. Min. Geochem., Min. Soc. Am. 87, 55–102.
Langdon, T.G., 2006. Grain boundary sliding revisited: developments in sliding over four decades. J. Mater. Sci. 41 (3), 597–609.
Mainprice, D., Bascou, J., Cordier, P., Tommasi, A., 2004. Crystal preferred orientations of garnet: comparion between numerical simulations and electron back-scattered diffraction (EBSD) measurements in naturally deformed eclogites. J. Struct. Geol. 26, 2089–2102.
Manning, C.E., 1994. The solubility of quartz in H2O in the lower crust and upper mantle. Geochem. Cosmochim. Acta 58 (22), 4831–4839.
Manning, C.E., 2004. The chemistry of subduction-zone fluids. Earth Planet Sci. Lett. 223 (1–2), 1–16.
Mansard, N., Stünitz, H., Raimbourg, H., Précigout, J., 2020. The role of deformation-reaction interactions to localize strain in polymineralic rocks: insights from experimentally deformed plagioclase-pyroxene assemblages. J. Struct. Geol. 134, 104008.
Marti, S., Stünitz, H., Heilbronner, R., Plümper, O., Drury, M., 2017. Experimental investigation of the brittle-viscous transition in mafic rocks–Interplay between fracturing, reaction, and viscous deformation. J. Struct. Geol. 105, 62–79.
Marti, S., Stünitz, H., Heilbronner, R., Plümper, O., Kilian, R., 2018. Syn-kinematic hydration reactions, grain size reduction, and dissolution-precipitation creep in experimentally deformed plagioclase-pyroxene mixtures. Solid Earth 9 (4), 985–1009.
Massey, M.A., Prior, D.J., Moecher, D.P., 2011. Microstructure and crystallographic preferred orientation of polycrystalline microgarnet aggregates developed during progressive creep, recovery, and grain boundary sliding. J. Struct. Geol. 33 (4), 713–730.
Masur, S., Aleksandrowski, P., 2001. The Tepla/Saxothuringian suture in the Karkonosze–Izera Massif, Western Sudetes, Central European Variscides. Int. J. Earth Sci. 90, 341–360.
Matte, P.H., Maluski, H., Rajlich, P., Franke, W., 1990. Terrane boundaries in the Bohemian Massif: result of large-scale Variscan shearing. Tectonophysics 177, 151–170.
Mauler, A., Godard, G., Kunze, K., 2001. Crystallographic fabrics of omphacite, rutile and quartz in Vendée eclogites (Aremorican Massif, France). Consequences for deformation mechanismns and regimes. Tectonophysics 342, 81–112.
Menegon, L., Stünitz, H., Nasipuri, P., Heilbronner, R., Svahnberg, H., 2013. Transition from fracturing to viscous flow in granulite facies perthitic feldspar (Lofoten, Norway). J. Struct. Geol. 48, 95–112.
Menegon, L., Fusseis, F., Stünitz, H., Xiao, X., 2015. Creep cavitation bands control porosity and fluid flow in lower crustal shear zones. Geology 43 (3), 227–230.
Misch, P., 1969. Paracrystalline microboudinage of zoned grains and other criteria for synkinematic growth of metamorphic minerals. Am. J. Sci. 267 (1), 43–63.
Moghadam, R.H., Trepmann, C.A., Stöckhert, B., Renner, J., 2010. Rheology of synthetic omphacite aggregates at high pressure and high temperature. J. Petrol. 51 (4), 921–945.
Müller, W.F., Franz, G., 2008. TEM-microstructures in omphacite and other minerals from eclogite near to a thrust zone; the Eclogite Zone–Venediger nappe area, Tauern Window, Austria. Neues Jahrbuch Mineral. Abhand.: J Mineral and Geochem 184 (3), 285–298.
Müller, W.F., Brenker, F.E., Barnert, E.B., Franz, G., 2004. Chain multiplicity faults in deformed omphacite from eclogite. Eur. J. Mineral 16 (1), 37–48.
Müller, W.F., Walte, N., Miyajima, N., 2008. Experimental deformation of ordered natural omphacite: a study by transmission electron microscopy. Eur. J. Mineral 20 (5), 835–844.
Nasdala, L., Massone, H.-J., 2000. Microdiamonds from the saxonian Erzgebirge, Germany. Eur. J. Mineral 12, 495–498.

Neufeld, K., Ring, U., Heidelbach, F., Dietrich, S., Neuser, R.D., 2008. Omphacite textures in eclogites of the tauern window: implications for the exhumation of the eclogite zone, eastern Alps. J. Struct. Geol. 30, 976–992.
O'Brien, P.J., 2000. The fundamental Variscan problem: high-temperature metamorphism at different depths and high-pressure metamorphism at different temperatures. Geol Soc London, Special Publ 179, 369–386.
Okudaira, T., Jeřábek, P., Stünitz, H., Fusseis, F., 2015. High-temperature fracturing and subsequent grain-size-sensitive creep in lower crustal gabbros: evidence for coseismic loading followed by creep during decaying stress in the lower crust? J. Geophys. Res.: Solid Earth 120 (5), 3119–3141.
Orzol, J., Trepmann, C.A., Stöckhert, B., Shi, G., 2003. Critical shear stress for mechanical twinning of jadeite—an experimental study. Tectonophysics 372 (3–4), 135–145.
Pacheco, J.F., Sykes, L.R., Scholz, C.H., 1993. Nature of seismic coupling along simple plate boundaries of the subduction type. J. Geophys. Res.: Solid Earth 98 (B8), 14133–14159.
Panozzo, R., 1984. Two-dimensional strain from the orientation of lines in a plane. J. Struct. Geol. 6, 215–221.
Phillipot, P., van Roermnund, H.L.M., 1992. Deformation processes in eclogitic rocks: evidence for rheological delamination oft he oceanic crust in deep levels of subdution zones. J. Struct. Geol. 14, 1059–1077.
Piepenbreier, D., Stöckhert, B., 2001. Plastic flow of omphacite in eclogites at temperatures below 500 C–implications for interplate coupling in subduction zones. Int. J. Earth Sci. 90 (1), 197–210.
Précigout, J., Stünitz, H., 2016. Evidence of phase nucleation during olivine diffusion creep: a new perspective for mantle strain localisation. Earth Planet Sci. Lett. 455, 94–105.
Putnis, A., 2009. Mineral replacement reactions. Rev. Mineral. Geochem. 70, 87–124.
Putnis, A., 2015. Transient porosity resulting from fluid–mineral interaction and its consequences. Rev. Mineral. Geochem. 80, 1–23.
Rehman, H.U., Mainprice, D., Barou, F., Yamamoto, H., Okamoto, K., 2016. EBSD-measured crystal preferred orientation of eclogites from the Sanbagawa metamorphic belt, central Shikoku, SW Japan. Eur. J. Mineral 28, 1155–1168.
Rybacki, E., Wirth, R., Dresen, G., 2008. High-strain creep of feldspar rocks: implications for cavitation and ductile failure in the lower crust. Geophys. Res. Lett. 35 (4).
Rötzler, K., Schumacher, R., Maresch, W.V., Willner, A.P., 1998. Characterization and geodynamic implications of contrasting metamorphic evolution in juxtaposed high-pressure units of the Western Erzgebirge (Saxony, Germany). Eur. J. Mineral 10, 261–280.
Schmädicke, E., Mezger, K., Cosca, M., Okrusch, M., 1995. Variscan Sm-Nd and Ar-Ar ages of eclogite facies rocks from the Erzgebirge, Bohemian Massif. J. Metamorph. Geol. 13, 537–552.
Schmid, S.M., Fügenschuh, B., Kissling, E., Schuster, R., 2004. Tectonic map and overall architecture of the Alpine orogen. Eclogae Geol. Helv. 97 (1), 93–117.
Schmid, S.M., Scharf, A., Handy, M.R., Rosenberg, C.L., 2013. The Tauern Window (Eastern Alps, Austria): a new tectonic map, with cross-sections and a tectonometamorphic synthesis. Swiss J. Geosci. 106 (1), 1–32.
Schulmann, K., Konopásek, J., Janoušek, V., Lexa, O., Lardeaux, J.M., Edel, J.B., Štípská, P., Ulrich, S., 2009. An andean type palaeozoic convergence in the bohemian massif. Compt. Rendus Geosci. 341, 266–286.
Schulmann, K., Lexa, O., Janoušek, V., Lardeaux, J.M., Edel, J.B., 2014. Anatomy of a diffuse cryptic suture zone: an example from the Bohemian Massif. European Variscides. Geol 42, 275–278.
Selverstone, J., 1993. Micro- to macro-scale interactions between deformation and metamorphism, tauern window, eastern Alps. Schweizerische Mineralogische und Petrographische Mitteilungen 73, 229–239.
Smit, M.A., Scherer, E.E., John, T., Janssen, A., 2011. Creep of garnet in eclogite: mechanisms and implications. Earth Planet Sci. Lett. 311 (3–4), 411–419.
Stöckhert, B., 2002. Stress and deformation in subduction zones: insight from the record of exhumed metamorphic rocks. Geol Soc London, Special Publ 200 (1), 255–274.
Stöckhert, B., Renner, J., 1998. Rheology of crustal rocks at ultrahigh pressure. In: When Continents Collide: Geodynamics and Geochemistry of Ultrahigh-Pressure Rocks. Springer, Dordrecht, pp. 57–95.
Stöckhert, B., Massonne, H.J., Nowlan, E.U., 1997. Low differential stress during high-pressure metamorphism: the microstructural record of a metapelite from the Eclogite Zone, Tauern Window, Eastern Alps. Lithos 41 (1–3), 103–118.
Storey, C.D., Prior, D.J., 2005. Plastic deformation and recrystallization of garnet: a mechanism to facilitate diffusion creep. J. Petrol. 46 (12), 2593–2613.
Stünitz, H., Tullis, J., 2001. Weakening and strain localization produced by syn-deformational reaction of plagioclase. Int. J. Earth Sci. 90 (1), 136–148.
Sundberg, M., Cooper, R.F., 2008. Crystallographic preferred orientation produced by diffusional creep of harzburgite: effects of chemical interactions among phases during plastic flow. J. Geophys. Res.: Solid Earth 113 (B12).
van Panhuys-Sigler, M., Hartman, P., 1981. Morphologie theoretique de certains pyroxenes deduite de la structure cristalline. Bull. Miner. 104, 95–106.
van Roermund, H., 1983. Petrofabrics and microstructures of omphacites in a high temperature eclogite from the Swedish Caledonides. Bull. Mineral. 106 (6), 709–713.
van Roermund, H.L., 1984. Omphacite microstructures from a Spanish eclogite. Texture, Stress, Microstruct. 6 (2), 105–116.
van Roermund, H.L.M., Boland, J.N., 1981. The dislocation substructures of naturally deformed omphacites. Tectonophysics 78 (1–4), 403–418.
Wassmann, S., Stöckhert, B., 2013. Rheology of the plate interface—dissolution precipitation creep in high pressure metamorphic rocks. Tectonophysics 608, 1–29.
Willner, A.P., Rötzler, K., Maresch, W.V., 1997. Pressure–temperature and fluid evolution of quartzo–feldspathic metamorphic rocks with a relic high-pressure, granulite-facies history from the Central Erzgebirge (Saxony, Germany). J. Petrol. 38, 307–336.
Zhang, J., Green, H.W., 2007. Experimental investigation of eclogite rheology and its fabrics at high temperature and pressure. J. Metamorph. Geol. 25 (2), 97–115.
Zhang, J., Green II, H.W., Bozhilov, K.N., 2006. Rheology of omphacite at high temperature and pressure and significance of its lattice preferred orientations. Earth Planet Sci. Lett. 246 (3–4), 432–443.
Zhao, Z.Y., Wei, C.J., Fang, A.M., 2005. Plastic flow of coesite eclogite in a deep continent subduction regime: microstructures, deformation mechanisms and rheologic implications. Earth Planet Sci. Lett. 237 (1–2), 209–222.
Zulauf, G., Dörr, W., Fiala, J., Kotková, J., Maluski, H., Valverde-Vaquero, P., 2002. Evidence for high-temperature diffusional creep preserved by rapid cooling of lower crust (North Bohemian shear zone, Czech Republic). Terra. Nova 14, 343–354.